Supporting Information

Oxidative Addition of Diaryldichalcogenides to the Diferrocenylphosphenium Ion: Synthesis, Structure and Organocatalytic Activity

Corina Stoian,[a†] Nils Schmidt,[a†] Thomas J. Kuczmera,[b] Pim Puylaert,[a] Enno Lork,[a]

Boris J. Nachtsheim,[*b] Emanuel Hupf,[*a] Jens Beckmann[*a]

[a]*Institut für Anorganische Chemie und Kristallographie, Universität Bremen, Leobener Str. 7, 28359 Bremen*

[b]*Institut für Organische und Analytische Chemie, Universität Bremen, Leobener Str. 7, 28359 Bremen*

Table of Contents

1 Experimental section

1.1 General Considerations

All the reactions, manipulations work-up and purifications were performed under inert argon atmosphere using anhydrous solvents. The reagents used in this work including Ph_2E_2 (E = S, Se, Te), 1-methylindole, *trans*-β-crotonophenone and Et_4Si were obtained commercially and used as received. $[Fc_2P][B(C_6F_5)_4]$,[S1] Fc_2Se_2[S2] and $biphenSe_2$ (dibenzo[1,2]diselenine),[S3] were prepared following the procedures described in the literature. Anhydrous dichloromethane, *n*-hexane, *n*-pentane and toluene were collected from an SPS800 mBraun solvent purification system and stored over 3 Å molecular sieves. Diethyl ether was dried by heating at reflux over Na/benzophenone under argon atmosphere. Deuterated solvents were degassed and dried over 3 Å molecular sieves under argon. Other solvents, such as 1,2-difluorobenzene, were dried directly over 3 Å molecular sieves.

Unless otherwise noted, NMR spectra were recorded at room temperature on a Bruker Avance Neo 600 MHz spectrometer. ^{1}H, $^{13}C\{^{1}H\}$, ^{11}B, ^{19}F, ^{31}P ^{77}Se and ^{125}Te NMR spectra are reported on the δ scale (ppm) and are referenced against $SiMe_4$, $BF_3{\cdot}Et_2O$ (15% in $CDCl_3$), $CFCl_3$, H_3PO_4 (85% in water), Me_2Se and Me_2Te respectively. ^{1}H and $^{13}C\{^{1}H\}$ chemical shifts are referenced to the residual peak of the solvent ($CDHCl_2$ 5.32 ppm for CD_2Cl_2) in the ^{1}H NMR spectra, and to the peak of the deuterated solvent (CD_2Cl_2 53.84 ppm) in the $^{13}C\{^{1}H\}$ NMR spectra.[S4]

The ESI HRMS spectra were measured on a Bruker Impact II spectrometer. Dichloromethane or dichloromethane/acetonitrile solutions (c =$1{\cdot}10^{-5}$ mol·L^{-1}) were injected directly into the spectrometer at a flow rate of 3 µL·min^{-1}. Nitrogen was used both as a drying gas and for nebulization with flow rates of approximately 5 L·min^{-1} and a pressure of 5 psi. Pressure in the mass analyser region was usually about $1{\cdot}10^{-5}$ mbar. Spectra were collected for 1 min and averaged. The nozzle-skimmer voltage was adjusted individually for each measurement.

UV-Vis absorption spectra were recorded on a VWR UV-1600PC spectrophotometer, and analysed using Spectragryph software.[S5] Melting points were determined on a SCHORPP Gerätetechnik MPM−H3, using one end closed capillary tubes, the other end was closed with silicon grease.

1.2 Preparation of $[Fc_2P(SPh)_2][B(C_6F_5)_4]$ (1)

$[Fc_2P][B(C_6F_5)_4]$ (103 mg, 95.4 µmol, 1.0 eq.) and Ph_2S_2 (23 mg, 105 µmol, 1.1 eq.) were dissolved in dichloromethane (6 mL) and stirred for 48 h at 60 °C. The reaction mixture turned orange, and the solvent was evaporated to dryness. The dark yellow solid was washed with hexane (4 × 5 mL) and dried under reduced pressure. The title product was obtained as a yellow solid (120 mg, 92.4 µmol, 97%). Crystals of **1** were obtained by layering a CH_2Cl_2 solution with *n*-hexane (V:V, 1:3).

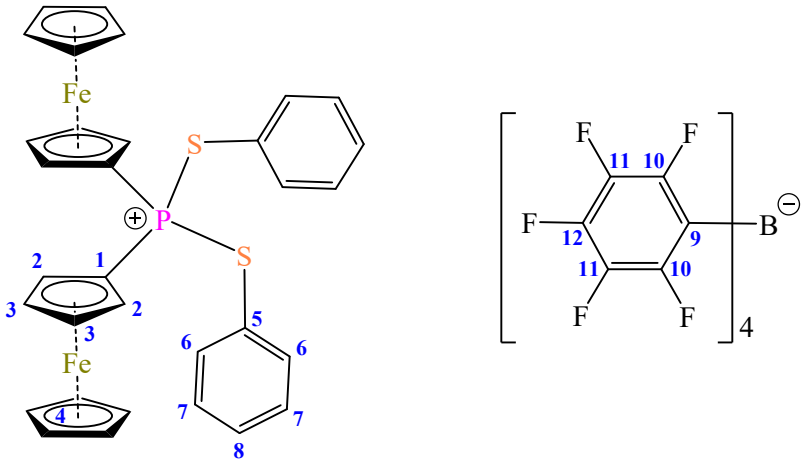

Figure S1. Numbering scheme for $[Fc_2P(SPh)_2][B(C_6F_5)_4]$ (**1**).

M.p. = 152–153 °C (decomp.) **^{1}H NMR (600 MHz, CD_2Cl_2):** δ (ppm) = 7.63 (t, $^1J(^1H–^1H)$ = 7 Hz, 2H, *H8*), 7.58 (d, $^1J(^1H–^1H)$ = 8 Hz, 4H, *H6*), 7.53 (t, $^1J(^1H–^1H)$ = 8 Hz, 4H, *H7*), 4.80 (s, br, 4H, *H3*), 4.50 (s, br, 4H, *H2*), 4.20 (s, 10H, *H4*). **^{13}C{^{1}H} NMR (151 MHz, CD_2Cl_2):** δ (ppm) = 148.6 (dm, $^1J(^{13}C–^{19}F)$ = 241 Hz, *C11*), 138.7 (dm, $^1J(^{13}C–^{19}F)$ = 245 Hz, *C12*), 137.8 (d, *C6*), 136.7 (dm, $^1J(^{13}C–^{19}F)$ = 245 Hz, *C10*), 132.8 (d, *C8*), 131.0 (s, *C7*), 124.4 (s, br, *C9*), 122.8 (d, $^1J(^{13}C–^{31}P)$ = 7 Hz, *C5*), 75.6 (d, $^3J(^{13}C–^{31}P)$ = 12 Hz, *C3*), 73.1 (d, $^2J(^{13}C–^{31}P)$ = 14 Hz, *C2*), 72.1 (s, *C4*), 64.4 ($^1J(^{13}C–^{31}P)$ = 99 Hz, *C1*). **^{19}F NMR (565 MHz, CD_2Cl_2):** δ = −133.1 (s, br, 8F, *F11*), −163.6 (t, $^3J(^{19}F–^{19}F)$ = 20 Hz, 4F, *F12*), −167.5 (t, $^3J(^{19}F–^{19}F)$ = 19 Hz, 8F, *F10*). **^{11}B NMR (193 MHz, CD_2Cl_2):** δ = −16.7 (s). **^{31}P{^{1}H} NMR (243 MHz, CD_2Cl_2):** δ (ppm) = 81.4 (s). **HRMS ESI** (m/z): $[M]^+$ calculated for $C_{32}H_{28}Fe_2PS_2$ 619.0063, found 619.0055.

1.3 Preparation of $[Fc_2P(SePh)_2][B(C_6F_5)_4]$ (2)

$[Fc_2P][B(C_6F_5)_4]$ (107 mg, 99.1 µmol, 1.0 eq.) and Ph_2Se_2 (34 mg, 109 µmol, 1.1 eq.) were combined in a Schlenk and dissolved in dichloromethane (6 mL). The reaction mixture was stirred for 3 h at room temperature for full conversion (orange solution). The solvent of was evaporated under reduced pressure and the solid was washed with hexane (4 × 5 mL). The title product was dried under vacuum and was obtained as an orange solid (110 mg, 78.9 µmol, 80%). Crystals of **2** were grown from a saturated solution in CH_2Cl_2 at −30 °C.

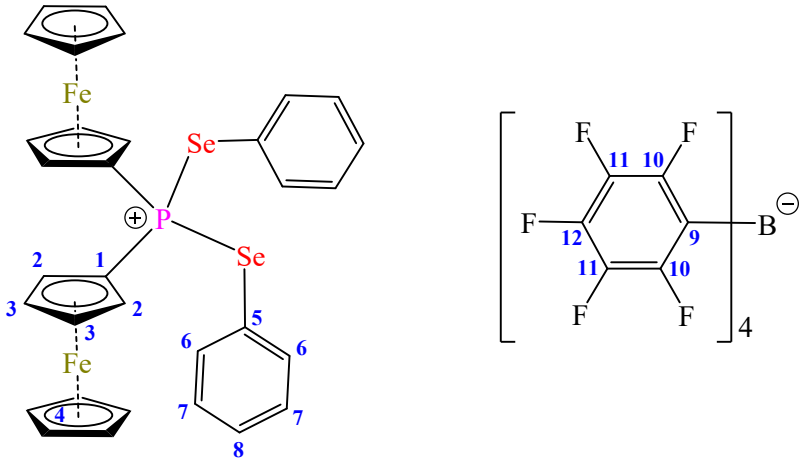

Figure S2. Numbering scheme for $[Fc_2P(SePh)_2][B(C_6F_5)_4]$(**2**).

M.p. = 191–192 °C. **^{1}H NMR (600 MHz, CD_2Cl_2):** δ (ppm) = 7.61 (m, 6H, *H8* and *H6*), 7.50 (t, 4H, *H7*), 4.80 (s, br, 4H, *H3*), 4.47 (s, br, 4H, *H2*), 4.18 (s, 10H, *H4*). **^{13}C{^{1}H} NMR (151 MHz, CD_2Cl_2):** δ (ppm) = 148.7 (dm, $^1J(^{13}C–^{19}F)$ = 241 Hz, *C11*), 138.8 (dm, $^1J(^{13}C–^{19}F)$ = 245 Hz, *C12*), 138.4 (d, $^4J(^{13}C–^{31}P)$ = 4Hz, *C7*), 136.9 (dm, $^1J(^{13}C–^{19}F)$ = 245 Hz, *C10*), 132.5 (d, $^5J(^{13}C–^{31}P)$ = 3 Hz, *C8*), 131.1 (d, $^3J(^{13}C–^{31}P)$ = 3 Hz, *C6*), 124.6 (s, br, *C9*), 122.8 (d, $^1J(^{13}C–^{77}Se)$ = 6 Hz, *C5*), 75.4 (d, $^3J(^{13}C–^{31}P)$ = 11 Hz, *C3*), 73.3 (d, $^2J(^{13}C–^{31}P)$ = 14 Hz, *C2*), 72.0 (s, *C4*), 66.3 (d, $^1J(^{13}C–^{31}P)$ = 78 Hz, *C1*). **^{11}B NMR (193 MHz, CD_2Cl_2):** δ (ppm) = 16.6 (s). **^{19}F NMR (565 MHz, CD_2Cl_2):** δ (ppm) = −133.1 (s, br, 8F, *F11*), −163.7 (t, $^3J(^{19}F–^{19}F)$ = 20 Hz, 4F, *F12*), −167.5 (t, $^3J(^{19}F–^{19}F)$ = 19 Hz, 8F, *F10*). **^{31}P{^{1}H} NMR (243 MHz, CD_2Cl_2):** δ (ppm) = 57.0 (s, $^1J(^{31}P–^{77}Se)$ = 475 Hz). **^{77}Se NMR (114 MHz, CD_2Cl_2):** δ (ppm) = 399.2 (d, $^1J(^{77}Se–^{31}P)$ = 475 Hz). **HRMS ESI** (m/z): $[M]^+$ calculated for $C_{32}H_{28}Fe_2PSe_2$ 714.8952, found 714.8966.

1.4 Preparation of $[Fc_2P(TePh)_2][B(C_6F_5)_4]$ (3)

$[Fc_2P][B(C_6F_5)_4]$ (78 mg, 72.2 µmol, 1.0 eq.) and Te_2Ph_2 (32 mg, 78.2 µmol, 1.1 eq.) were dissolved in dichloromethane (6 mL) and stirred for 48 h at room temperature. (When the reaction is followed by NMR, the title product is formed immediately, but there is always a small residue of phosphenium left). The solvent was evaporated and the solid was washed with hexane (4 × 5 mL). The product was dried under vacuum to obtain a dark red solid (87 mg, 58.4 µmol, 81%). Crystals of **3** (bright red) were obtained by liquid-to-liquid diffusion at −30 °C (a solution of **3** in CH_2Cl_2 layered with *n*-pentane, V:V, 1:3).

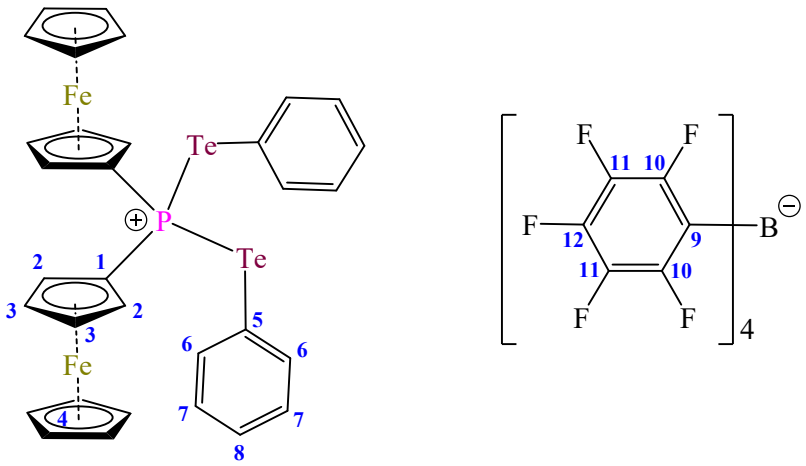

Figure S3. Numbering scheme for $[Fc_2P(TePh)_2][B(C_6F_5)_4]$(**3**).

M.p. = 149–150 °C (decomp.). **^{1}H NMR (600 MHz, CD_2Cl_2):** δ (ppm) = 7.80 (t, br, $^{3}J(^{1}H–^{1}H)$ = 9 Hz, 4H, *H6*), 7.61 (t, $^{3}J(^{1}H–^{1}H)$ = 7 Hz, 2H, *H8*), 7.43 (t, $^{3}J(^{1}H–^{1}H)$ = 8 Hz, 4H, *H7*), 4.78 (s, 4H, *H3*), 4.42 (s, 4H, *H2*), 4.17 (s, 10H, *H4*). **^{13}C{^{1}H} NMR (151 MHz, CD_2Cl_2):** δ (ppm) = 148.6 (dm, $^{1}J(^{13}C–^{19}F)$ = 242 Hz, *C11*), 142.4 (d, $^{3}J(^{13}C–^{31}P)$ = 2 Hz, *C6*), 138.7 (dm, $^{1}J(^{13}C–^{19}F)$ = 245 Hz, *C12*), 136.8 (dm, $^{1}J(^{13}C–^{19}F)$ = 246 Hz, *C10*), 132.3 (d, $^{5}J(^{13}C–^{31}P)$ = 3 Hz, *C8*), 131.4 (d, $^{4}J(^{13}C–^{31}P)$ = 3 Hz, *C7*), 75.0 (d, $^{3}J(^{13}C–^{31}P)$ = 10 Hz, *C3*), 74.0 (d, $^{2}J(^{13}C–^{31}P)$ = 13 Hz, *C2*), 71.7 (s, *C4*), 69.0 (d, $^{1}J(^{13}C–^{31}P)$ = 56 Hz, *C1*). **^{11}B NMR (193 MHz, CD_2Cl_2):** δ (ppm) = 16.7 (s). **^{19}F NMR (565 MHz, CD_2Cl_2):** δ (ppm) = −133.1 (s, br, 8F, *F11*), −163.7 (t, $^{3}J(^{19}F–^{19}F)$ = 20 Hz, 4F, *F12*), −167.5 (t, $^{3}J(^{19}F–^{19}F)$ = 19 Hz, 8F, *F10*). **^{31}P{^{1}H} NMR (243 MHz, CD_2Cl_2):** δ (ppm) = −22.8 (s, $^{1}J(^{31}P–^{125}Te)$ = 1041 Hz, $^{1}J(^{31}P–^{123}Te)$ = 870 Hz). **^{125}Te NMR (189 MHz, CD_2Cl_2):** δ (ppm) = 780.8 (d, $^{1}J(^{125}Te–^{31}P)$ = 1041 Hz). Attempted characterisation by high resolution mass spectrometry (ESI, APCI, LIFDI) was unsuccessful and yielded only decomposition fragments.

1.5 Preparation of $[Fc_2P(SeFc)_2][B(C_6F_5)_4]$ (4)

$[Fc_2P][B(C_6F_5)_4]$ (103 mg, 95.4 µmol, 1.0 eq.) and Fc_2Se_2 (56 mg, 106 µmol, 1.1 eq.) were dissolved in dichloromethane (6 mL) at −80 °C. The solution was stirred 48 h at room temperature. The solvent of the dark red solution was evaporated under vacuum and the solid was washed with *n*-hexane (4 × 5 mL). The solvent was removed under reduced pressure. The product was obtained as a red/ brown powder (138 mg, 85.8 µmol, 90%). Single crystals of the title product were obtained by layering a solution of **4** in dichloromethane with *n*-hexane at −30 °C.

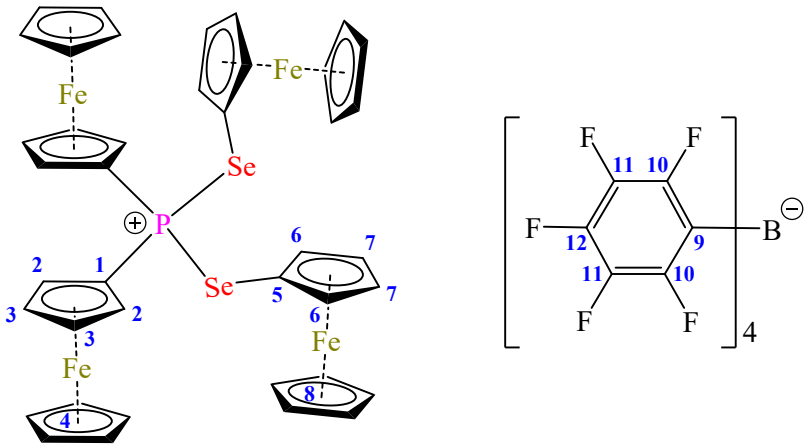

Figure S4. Numbering scheme for $[Fc_2P(SeFc)_2][B(C_6F_5)_4]$ (**4**).

M.p. = 158−159 °C. **^{1}H NMR (600 MHz, CD_2Cl_2):** δ (ppm) = 4.75 (s, 4H, *H3*), 4.50 (s, 4H, *H7*), 4.43 (s, 4H, *H2*), 4.37 (s, 4H, *H6*), 4.35 (s, 10H, *H4*), 4.20 (s, 10H, *H8*). **^{13}C{^{1}H} NMR (151 MHz, CD_2Cl_2):** δ (ppm) = 148.7 (dm, $^1J(^{13}C–^{19}F)$ = 240 Hz, *C11*), 138.8 (dm, $^1J(^{13}C–^{19}F)$ = 244 Hz, *C12*), 136.8 (dm, $^1J(^{13}C–^{19}F)$ = 245 Hz, *C10*), 124.6 (s, br, *C9*), 76.8 (s, *C7*), 74.9 (d, $^3J(^{13}C–^{31}P)$ = 11 Hz, *C3*), 73.3 (d, $^2J(^{13}C–^{31}P)$ = 13 Hz, *C2*), 72.8 (s, *C6*), 71.7 (s, *C4*), 70.8 (s, *C8*), 66.3 (d, $^1J(^{13}C–^{31}P)$ = 70 Hz, *C1*), 65.9 (s, *C5*). **^{11}B NMR (193 MHz, CD_2Cl_2):** δ (ppm) = 17.2 (s). **^{19}F NMR (565 MHz, CD_2Cl_2):** δ (ppm) = −133.9 (s, br, 8F, *F11*), −164.0 (t, $^3J(^{19}F–^{19}F)$ = 20 Hz, 4F, *F12*), −168.2 (t, $^3J(^{19}F–^{19}F)$ = 16 Hz, 8F, *F10*). **^{31}P{^{1}H} NMR (243 MHz, CD_2Cl_2):** δ (ppm) = 47.5 (s, $^1J(^{31}P–^{77}Se)$ = 498 Hz). **^{77}Se NMR (114 MHz, CD_2Cl_2):** δ (ppm) = 325.7 (d, $^1J(^{77}Se–^{31}P)$ = 498 Hz). **HRMS ESI** (m/z): $[M]^+$ calculated for $C_{40}H_{36}Fe_4PSe_2$ 930.8277, found 930.8287.

1.6 Preparation of $[Fc_2P(Se_2biphen)][B(C_6F_5)_4]$ (5)

$[Fc_2P][B(C_6F_5)_4]$ (523 mg, 484 µmol, 1.0 eq.) and Se_2biphen (151 mg, 484 µmol, 1.0 eq.) were dissolved in dichloromethane (7 mL) at −80 °C, then the reaction mixture was stirred overnight at room temperature. The solvent of the dark yellow solution was removed under vacuum. The resulted brown oil was washed with hexane (4 × 5 mL), then dried under reduced pressure to obtain a yellow solid (465 mg, 334 µmol, 69%). Single crystals of the product were obtained by layering a solution of **5** in CH_2Cl_2 with *n*-hexane.

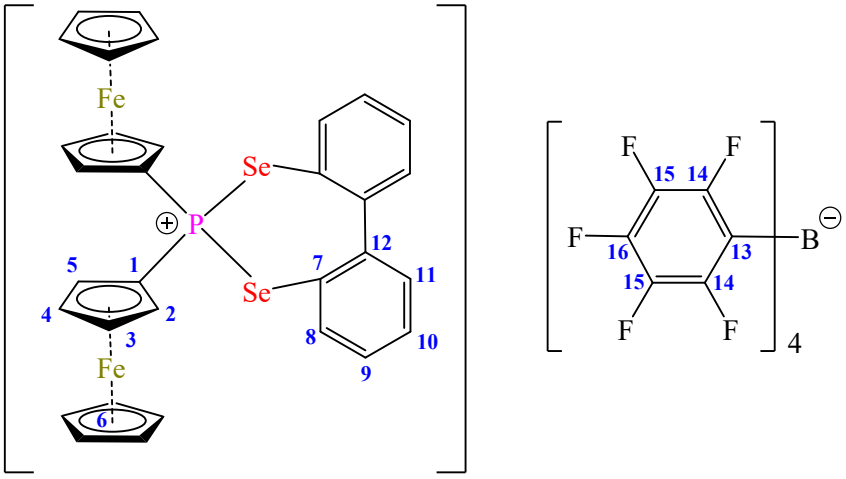

Figure S5. Numbering scheme for $[Fc_2P(Se_2biphen)][B(C_6F_5)_4]$ (**5**).

M.p. = 189–190 °C. **^{1}H NMR (600 MHz, CD_2Cl_2):** δ (ppm) = 7.76 (m, 2H, *H10*), 7.69 (d, 2H, *H8*), 7.60 (d, 2H, *H11*), 7.51 (t, 2H, *H9*), 4.93 (s, 2H), 4.85 (s, 2H), 4.82 (s, 2H), 4.30 (s, 10H, *H6*), 4.25 (s, 2H). **^{13}C{^{1}H} NMR (151 MHz, CD_2Cl_2):** δ (ppm) = 148.7 (dm, $^1J(^{13}C–^{19}F)$ = 241 Hz, *C15*), 146.7 (s, *C12*), 138.8 (dm, $^1J(^{13}C–^{19}F)$ = 245 Hz, *C16*), 138.3 (s, *C8*), 136.9 (dm, $^1J(^{13}C–^{19}F)$ = 245 Hz, *C14*), 133.2 (d, *C10*), 131.8 (d, *C11*), 130.7 (d, *C9*), 126.2 (d, *C7*), 124.4 (s, br, *C13*), 76.2 (d, $^3J(^{13}C–^{31}P)$ = 11 Hz), 75.4 (d, $^3J(^{13}C–^{31}P)$ = 12 Hz), 73.9 (d, $^2J(^{13}C–^{31}P)$ = 17 Hz), 72.9 (d, $^2J(^{13}C–^{31}P)$ = 13 Hz), 72.2 (s, *C6*), 64.2 (d, $^1J(^{13}C–^{31}P)$ = 77 Hz, *C1*).**^{11}B NMR (193 MHz, CD_2Cl_2):** δ (ppm) = 16.6 (s). **^{19}F NMR (565 MHz, CD_2Cl_2):** δ (ppm) = −133.0 (s, br, 8F, *F15*), −163.5 (t, $^3J(^{19}F–^{19}F)$ = 20 Hz, 4F, *F16*), −167.4 (t, $^3J(^{19}F–^{19}F)$ = 19 Hz, 8F, *F14*). **^{31}P{^{1}H} NMR (243 MHz, CD_2Cl_2):** δ (ppm) = 74.9 (s, $^1J(^{31}P–^{77}Se)$ = 444 Hz). **^{77}Se NMR (114 MHz, CD_2Cl_2):** δ (ppm) = 378.8 (d, $^1J(^{77}Se–^{31}P)$ = 444 Hz). **HRMS ESI** (m/z): $[M]^+$ calculated for $C_{32}H_{26}Fe_2PSe_2$ 712.8796, found 712.8785.

2 NMR Spectra

2.1 $[Fc_2P(SPh)_2][B(C_6F_5)_4]$ (1)

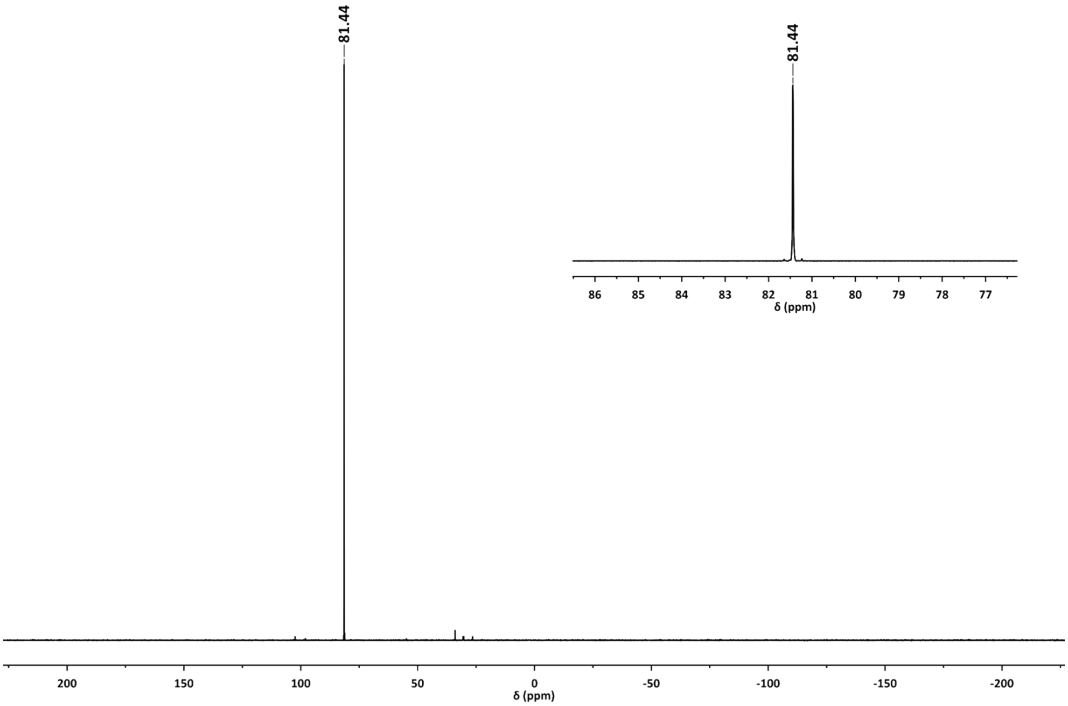

Figure S6. $^{31}P\{^1H\}$ NMR (CD_2Cl_2, 243 MHz) spectrum of $[Fc_2P(SPh)_2][B(C_6F_5)_4]$ (**1**).

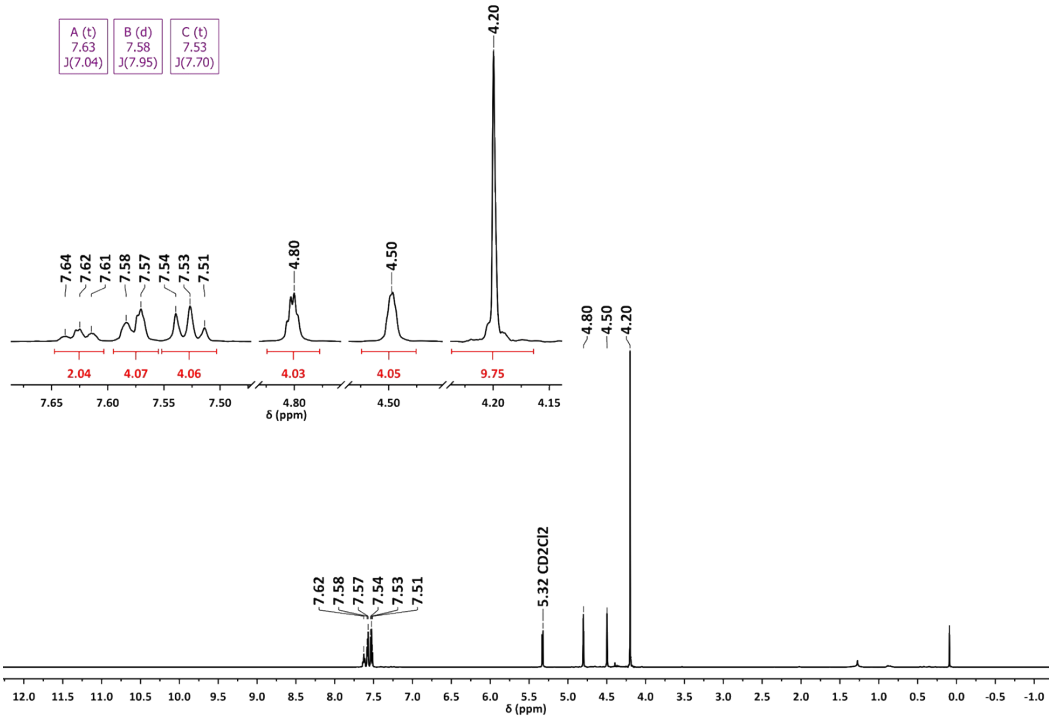

Figure S7. ^1H NMR (CD_2Cl_2, 600 MHz) spectrum of $[Fc_2P(SPh)_2][B(C_6F_5)_4]$ (**1**).

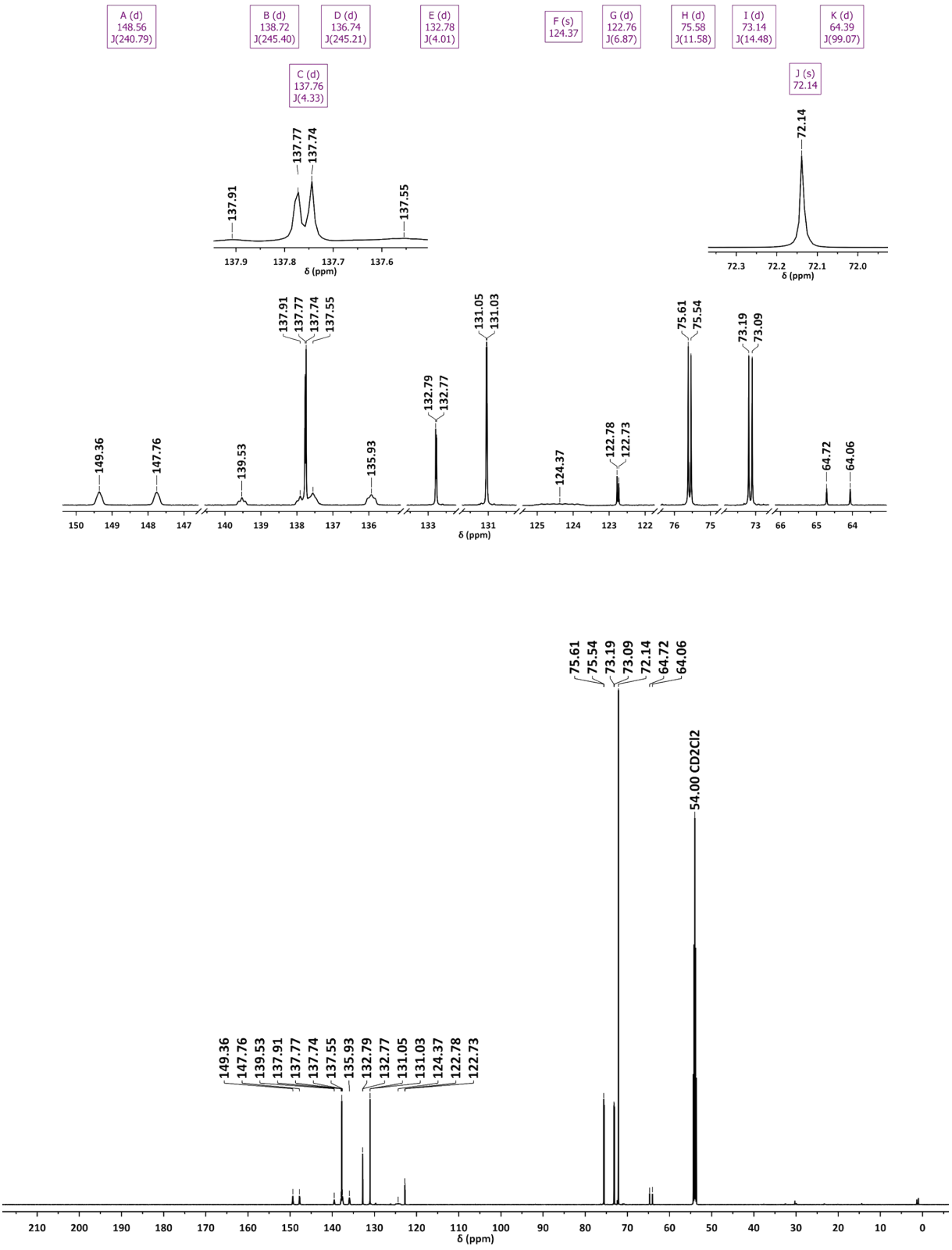

Figure S8. $^{13}C\{^{1}H\}$ NMR (CD_2Cl_2, 151 MHz) spectra of $[Fc_2P(SPh)_2][B(C_6F_5)_4]$ (**1**).

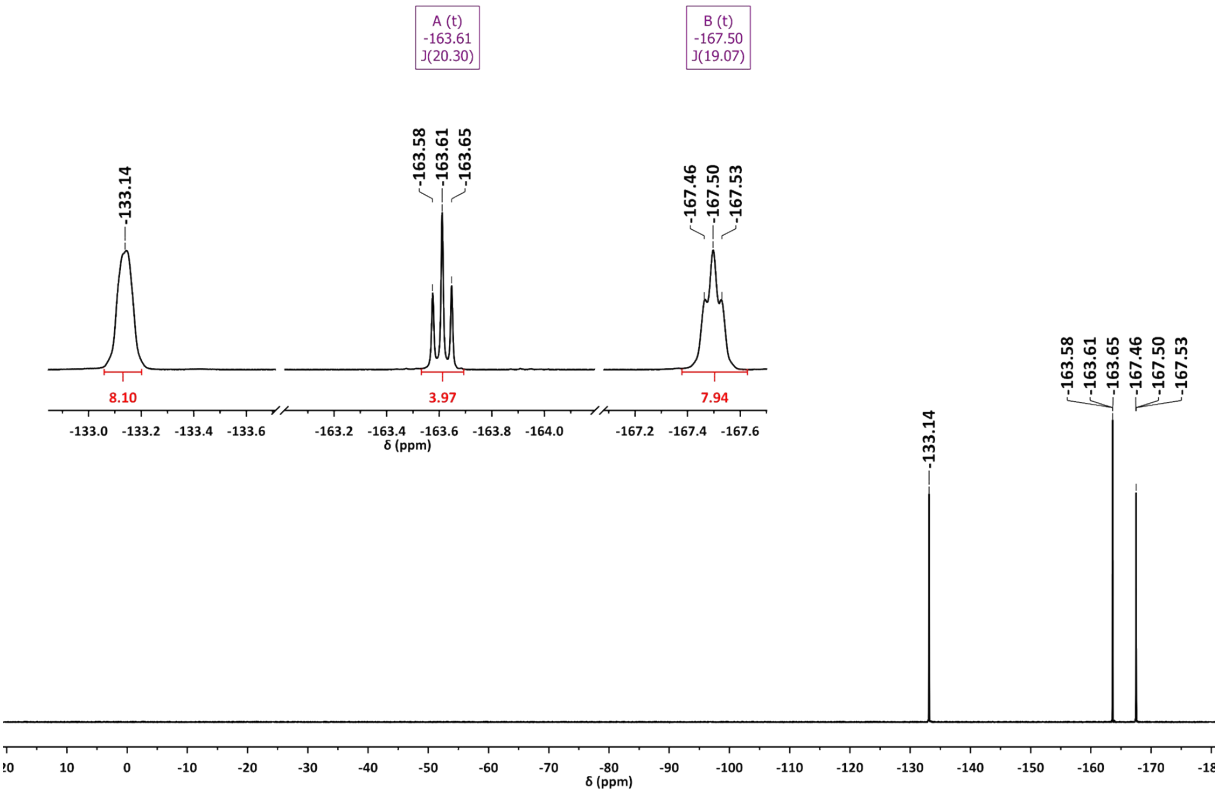

Figure S9. ^{19}F NMR (CD_2Cl_2, 565 MHz) spectrum of $[Fc_2P(SPh)_2][B(C_6F_5)_4]$ (**1**).

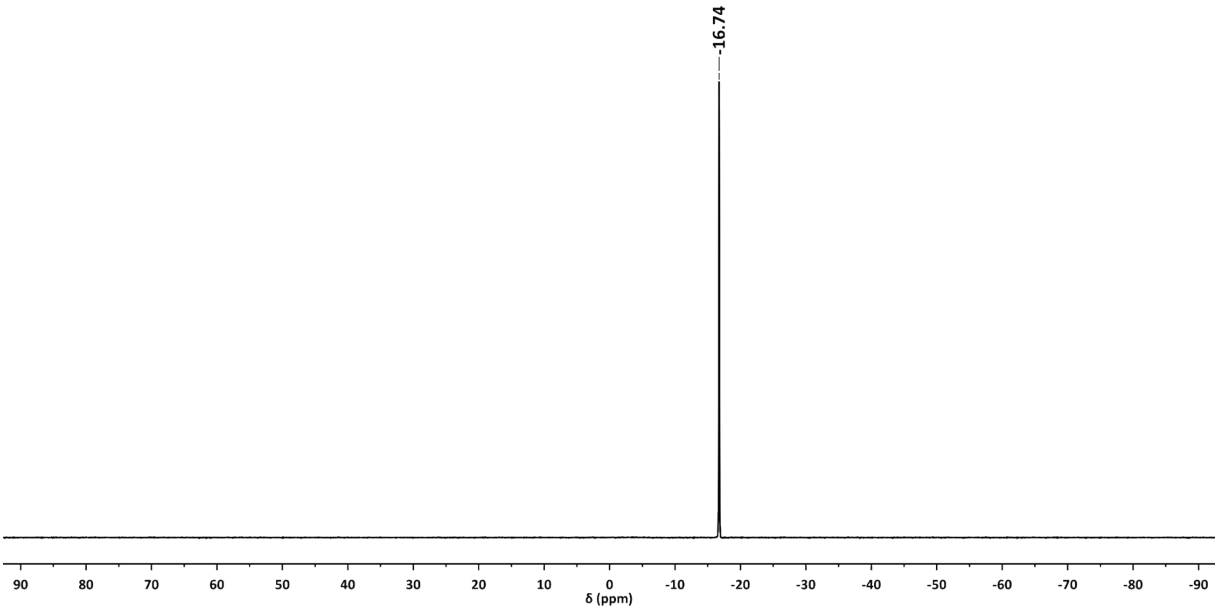

Figure S10. ^{11}B NMR (CD_2Cl_2, 193 MHz) spectrum of $[Fc_2P(SPh)_2][B(C_6F_5)_4]$ (**1**).

2.2 $[Fc_2P(SePh)_2][B(C_6F_5)_4]$ (2)

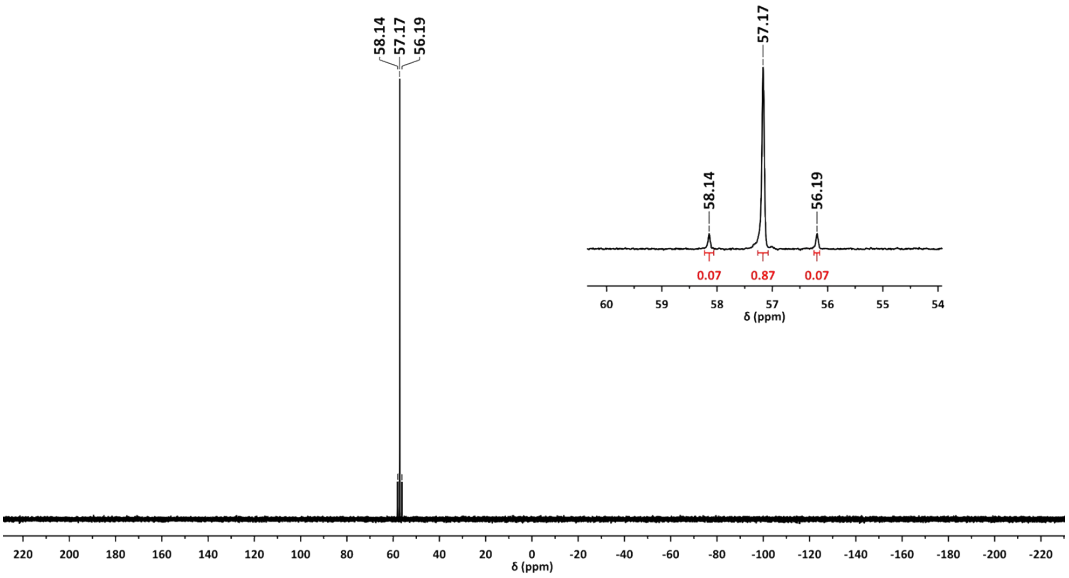

Figure S11. ^{31}P NMR (CD_2Cl_2, 243 MHz) spectrum of $[Fc_2P(SePh)_2][B(C_6F_5)_4]$ (**2**).

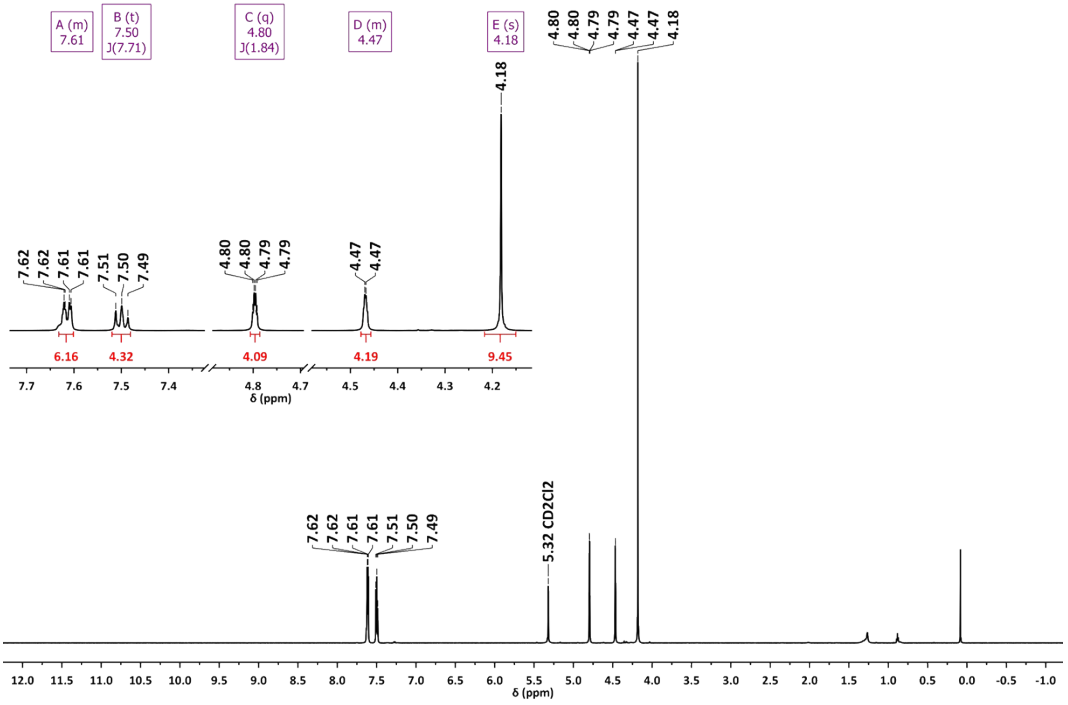

Figure S12. ^{1}H NMR (CD_2Cl_2, 600 MHz) spectrum of $[Fc_2P(SePh)_2][B(C_6F_5)_4]$ (**2**).

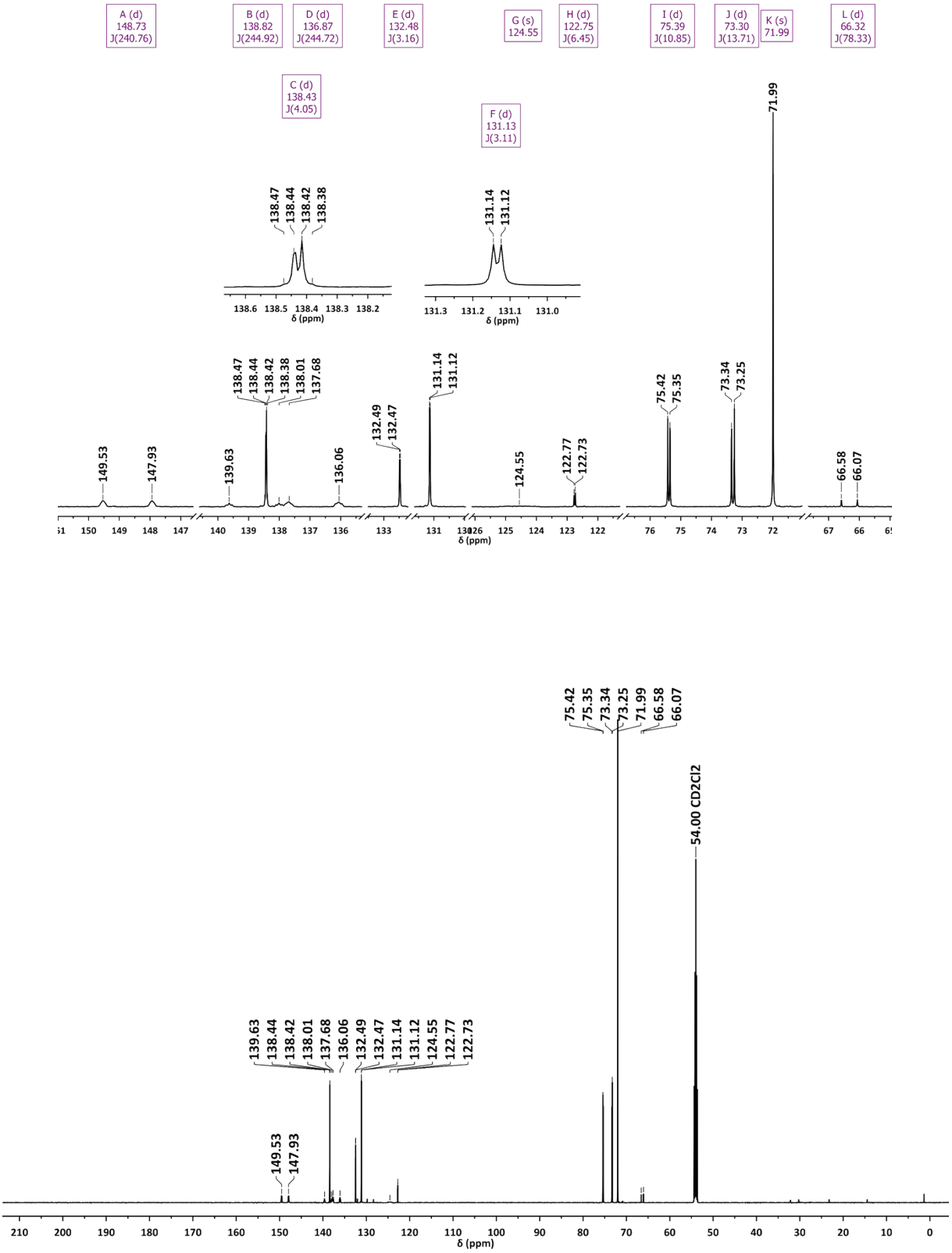

Figure S13. $^{13}C\{^{1}H\}$ NMR (CD_2Cl_2, 151 MHz) spectra of $[Fc_2P(SePh)_2][B(C_6F_5)_4]$ (**2**).

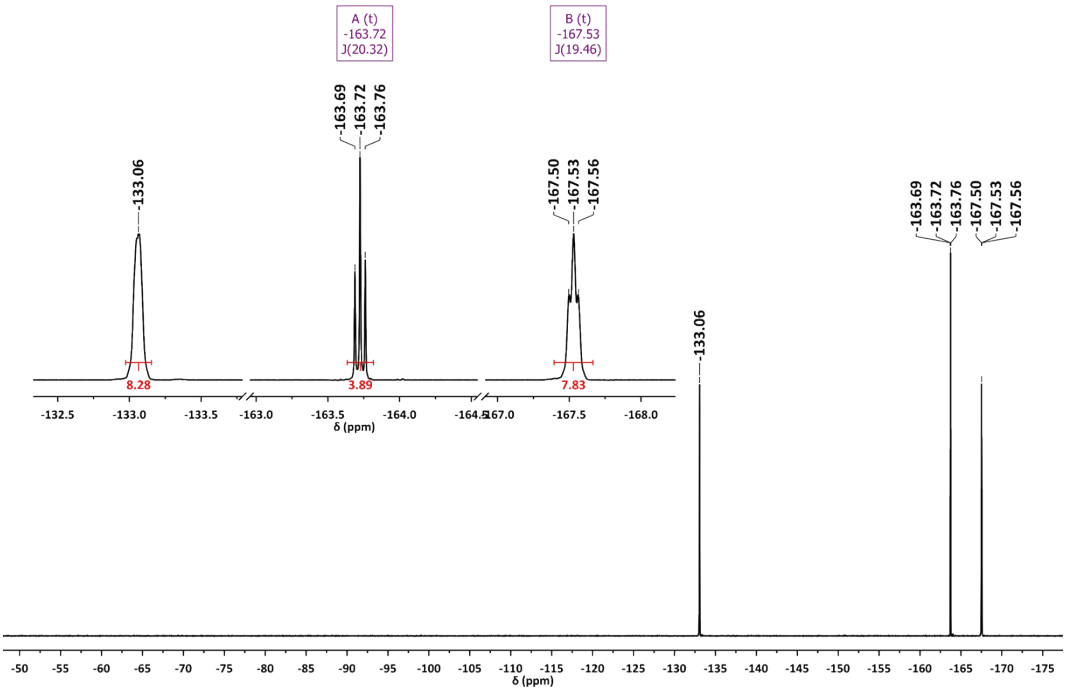

Figure S14. ^{19}F NMR (CD_2Cl_2, 565 MHz) spectrum of $[Fc_2P(SePh)_2][B(C_6F_5)_4]$ (**2**).

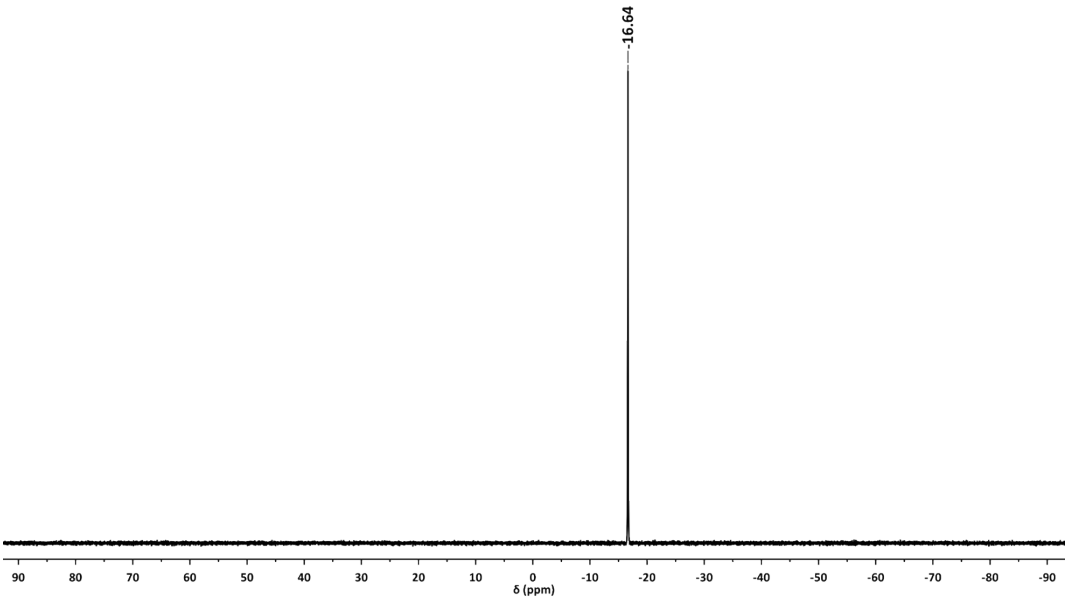

Figure S15. ^{11}B NMR (CD_2Cl_2, 193 MHz) spectrum of $[Fc_2P(SePh)_2][B(C_6F_5)_4]$ (**2**).

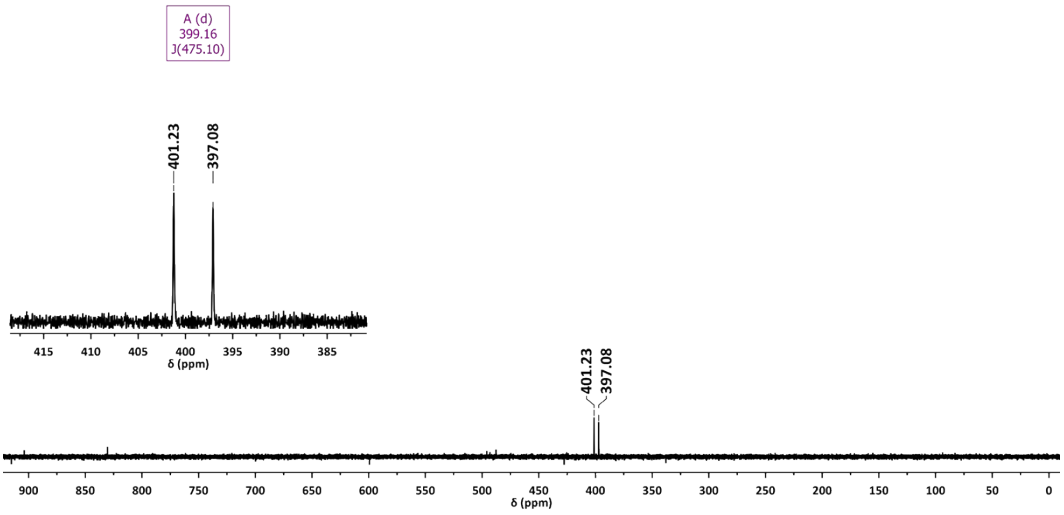

Figure S16. ^{77}Se NMR (CD_2Cl_2, 114 MHz) spectrum of $[Fc_2P(SePh)_2][B(C_6F_5)_4]$ (**2**).

2.3 $[Fc_2P(TePh)_2][B(C_6F_5)_4]$ (3)

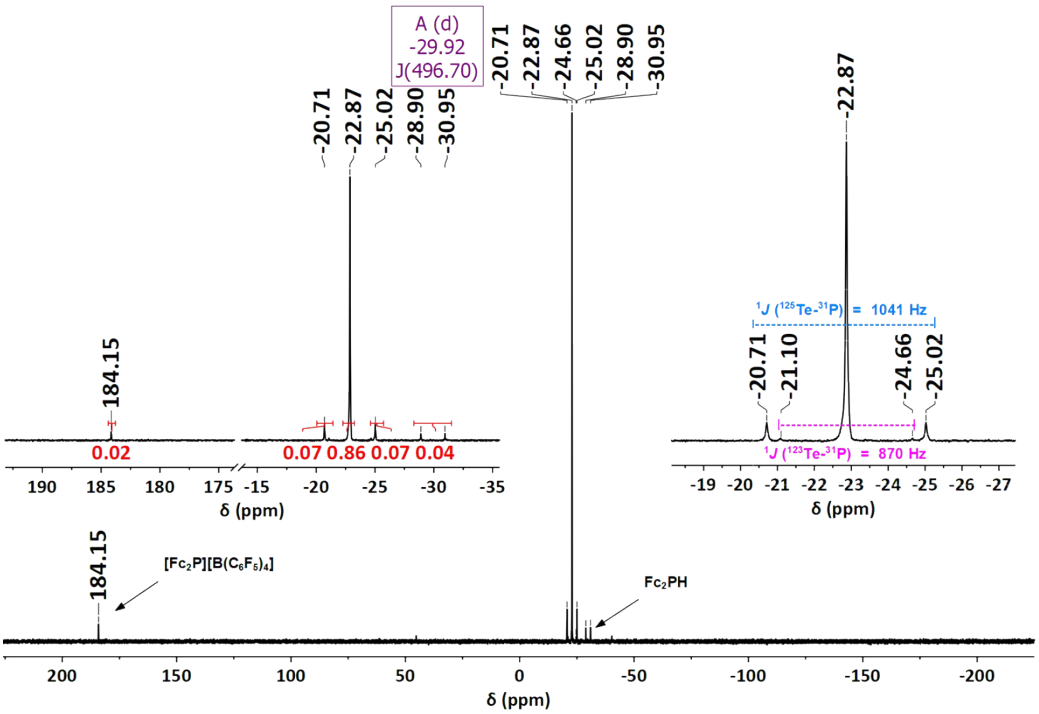

Figure S17. ^{31}P NMR (CD_2Cl_2, 243 MHz) spectrum of $[Fc_2P(TePh)_2][B(C_6F_5)_4]$ (**3**).

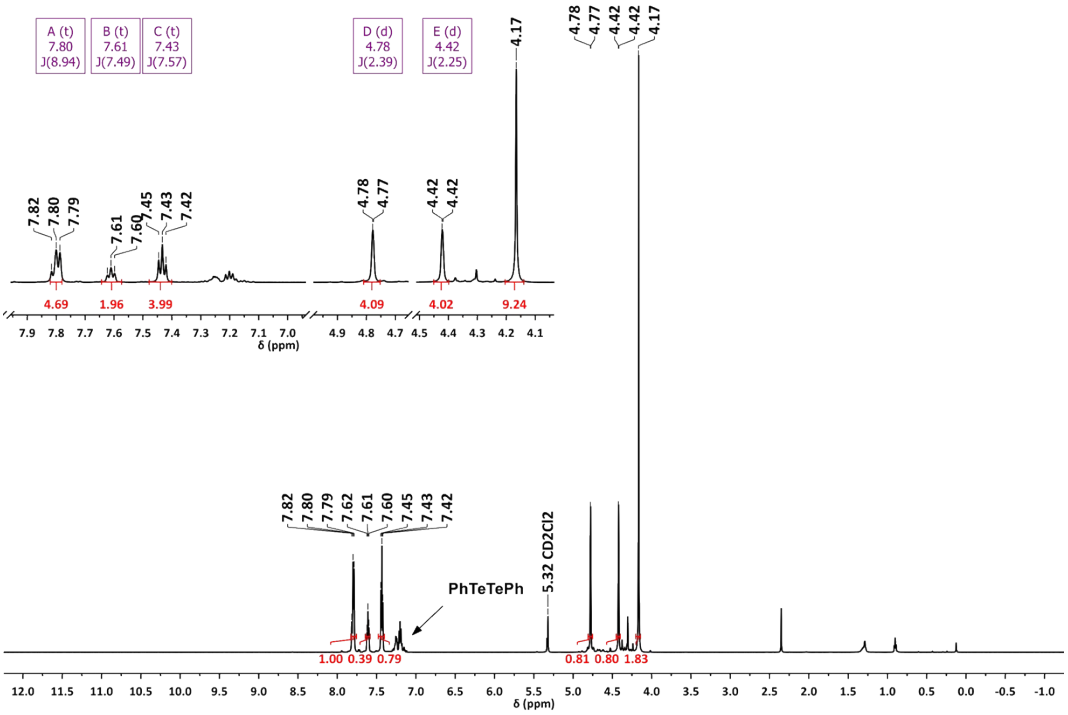

Figure S18. ^{1}H NMR (CD_2Cl_2, 600 MHz) spectrum of $[Fc_2P(TePh)_2][B(C_6F_5)_4]$ (**3**).

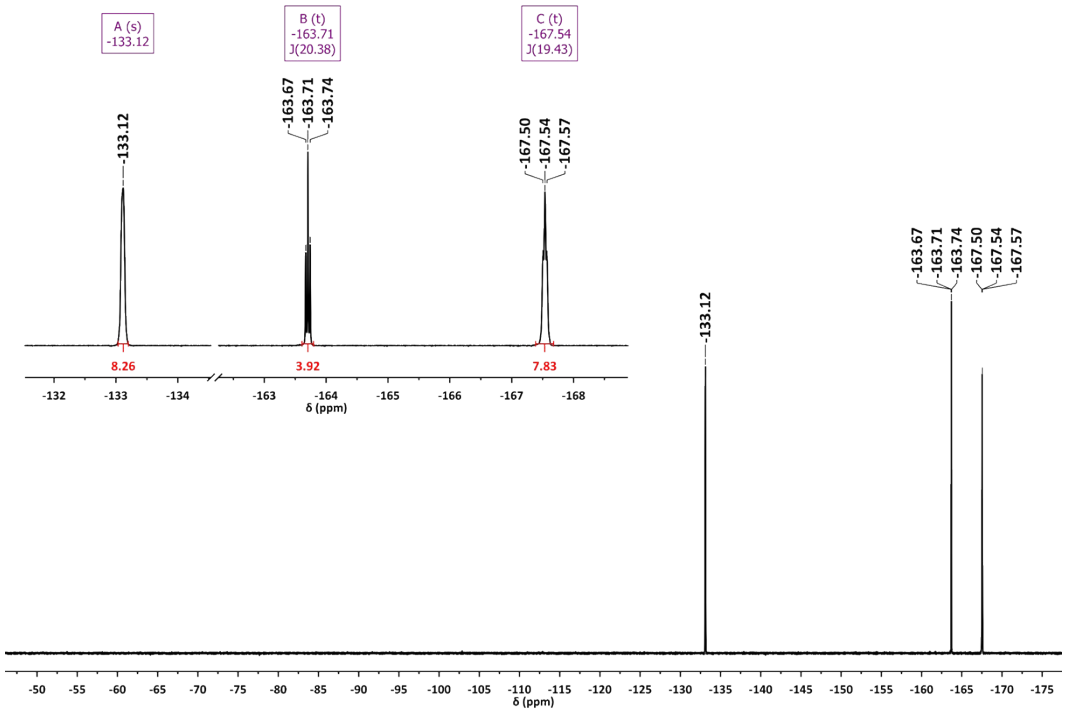

Figure S19. ^{19}F NMR (CD_2Cl_2, 565 MHz) spectrum of $[Fc_2P(TePh)_2][B(C_6F_5)_4]$ (**3**).

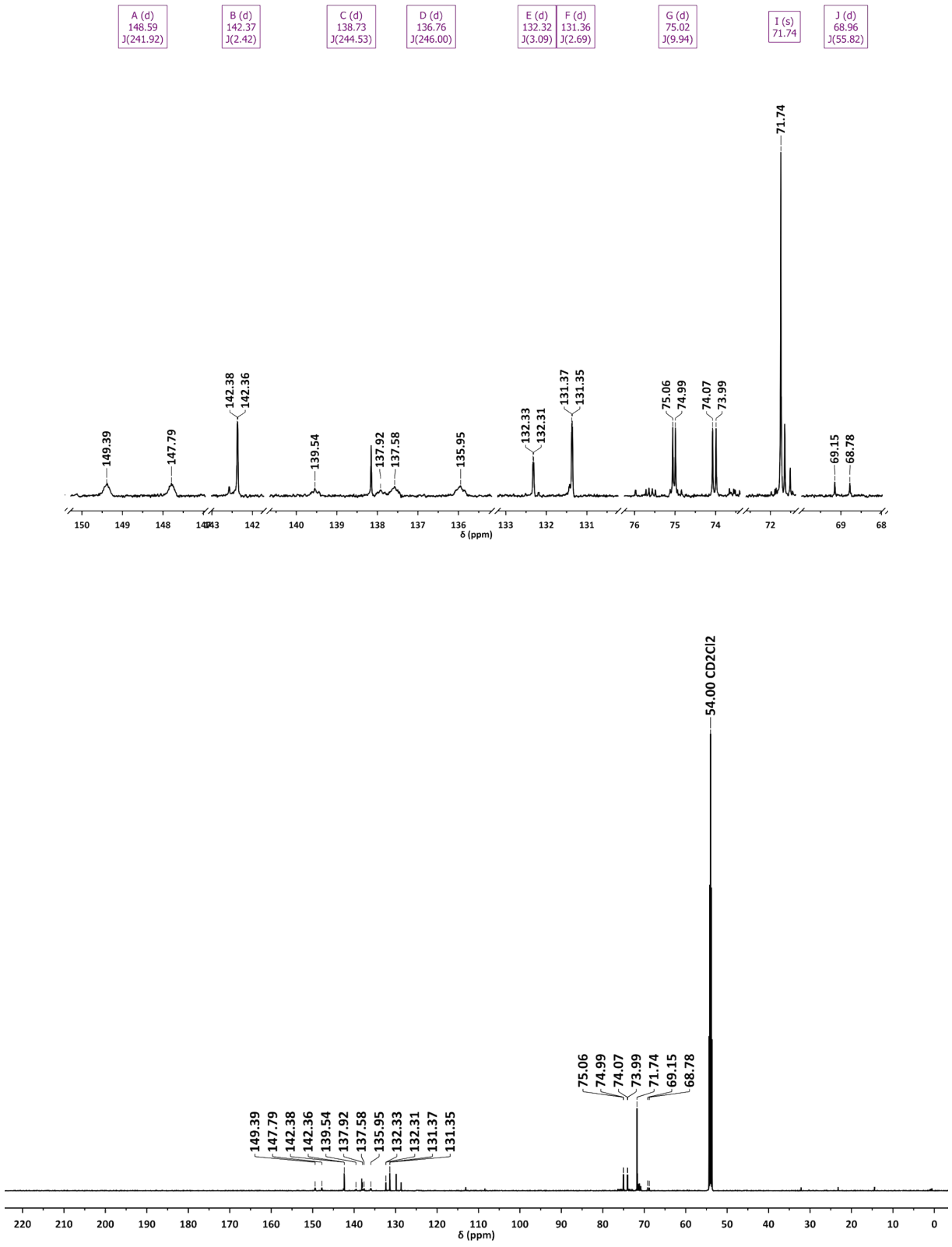

Figure S20. ^{13}C NMR (CD_2Cl_2, 151 MHz) spectra of $[Fc_2P(TePh)_2][B(C_6F_5)_4]$ (**3**).

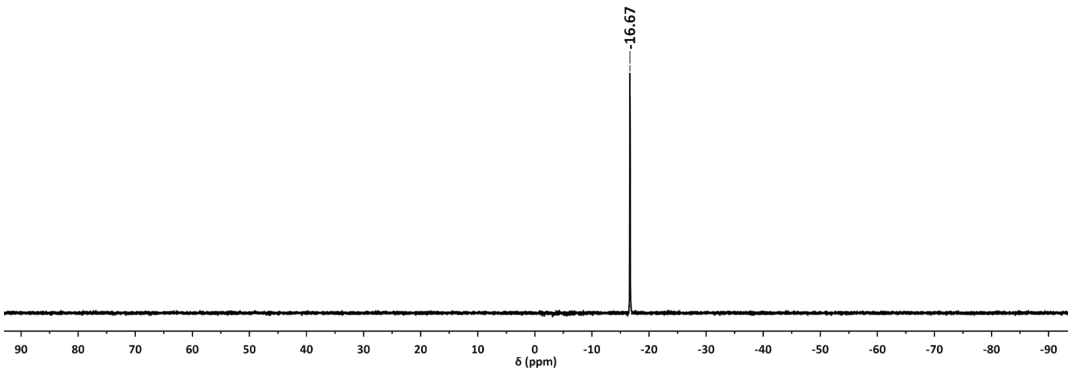

Figure S21. ^{11}B NMR (CD_2Cl_2, 193 MHz) spectrum of $[Fc_2P(TePh)_2][B(C_6F_5)_4]$ (**3**).

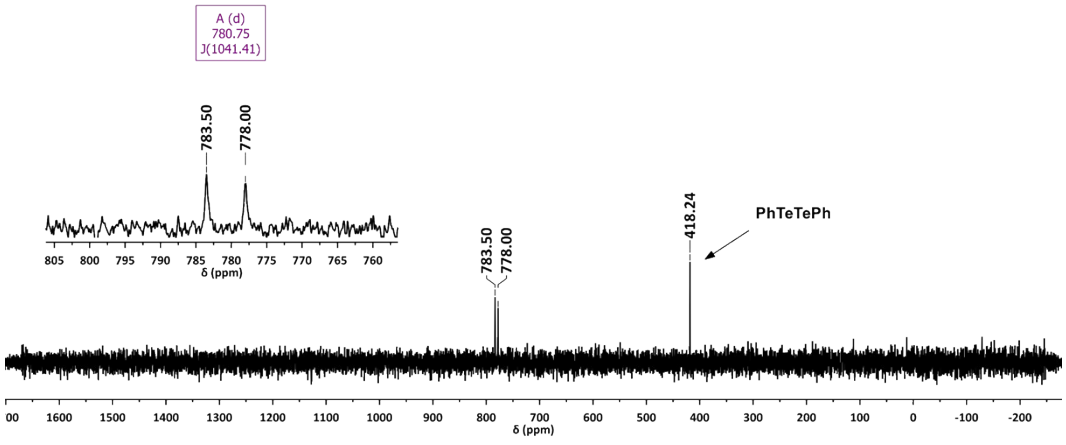

Figure S22. ^{125}Te NMR (CD_2Cl_2, 189 MHz) spectrum of $[Fc_2P(TePh)_2][B(C_6F_5)_4]$ (**3**).

2.4 $[Fc_2P(SeFc)_2][B(C_6F_5)_4]$ (4)

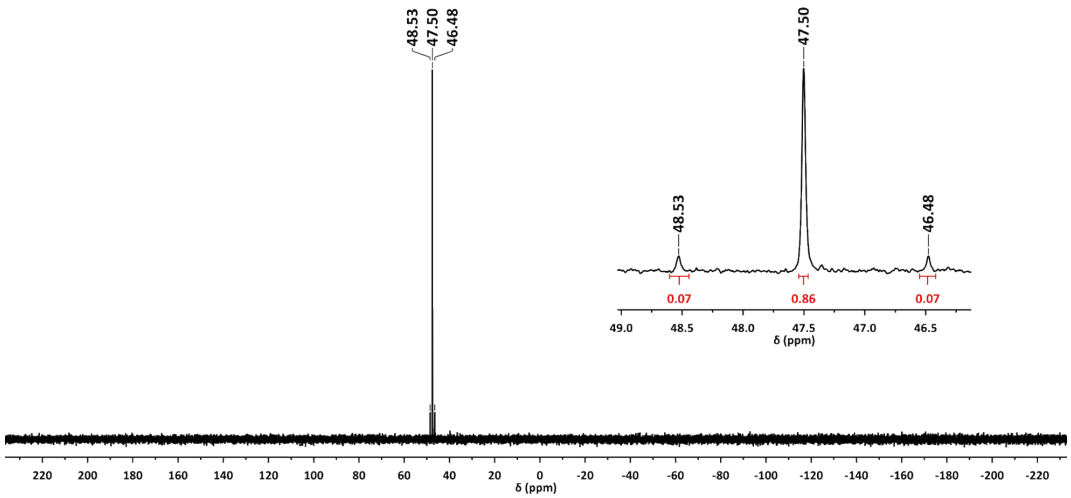

Figure S23. ^{31}P NMR (CD_2Cl_2, 243 MHz) spectrum of $[Fc_2P(SeFc)_2][B(C_6F_5)_4]$ (**4**).

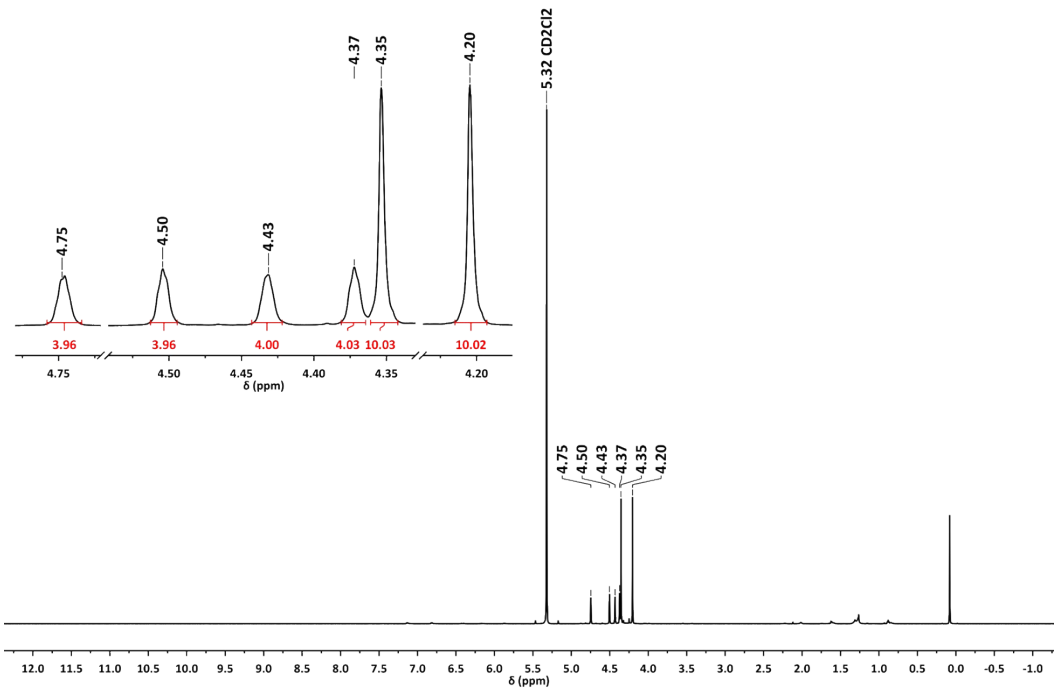

Figure S24. ^{1}H NMR (CD_2Cl_2, 600 MHz) spectrum of $[Fc_2P(SeFc)_2][B(C_6F_5)_4]$ (**4**).

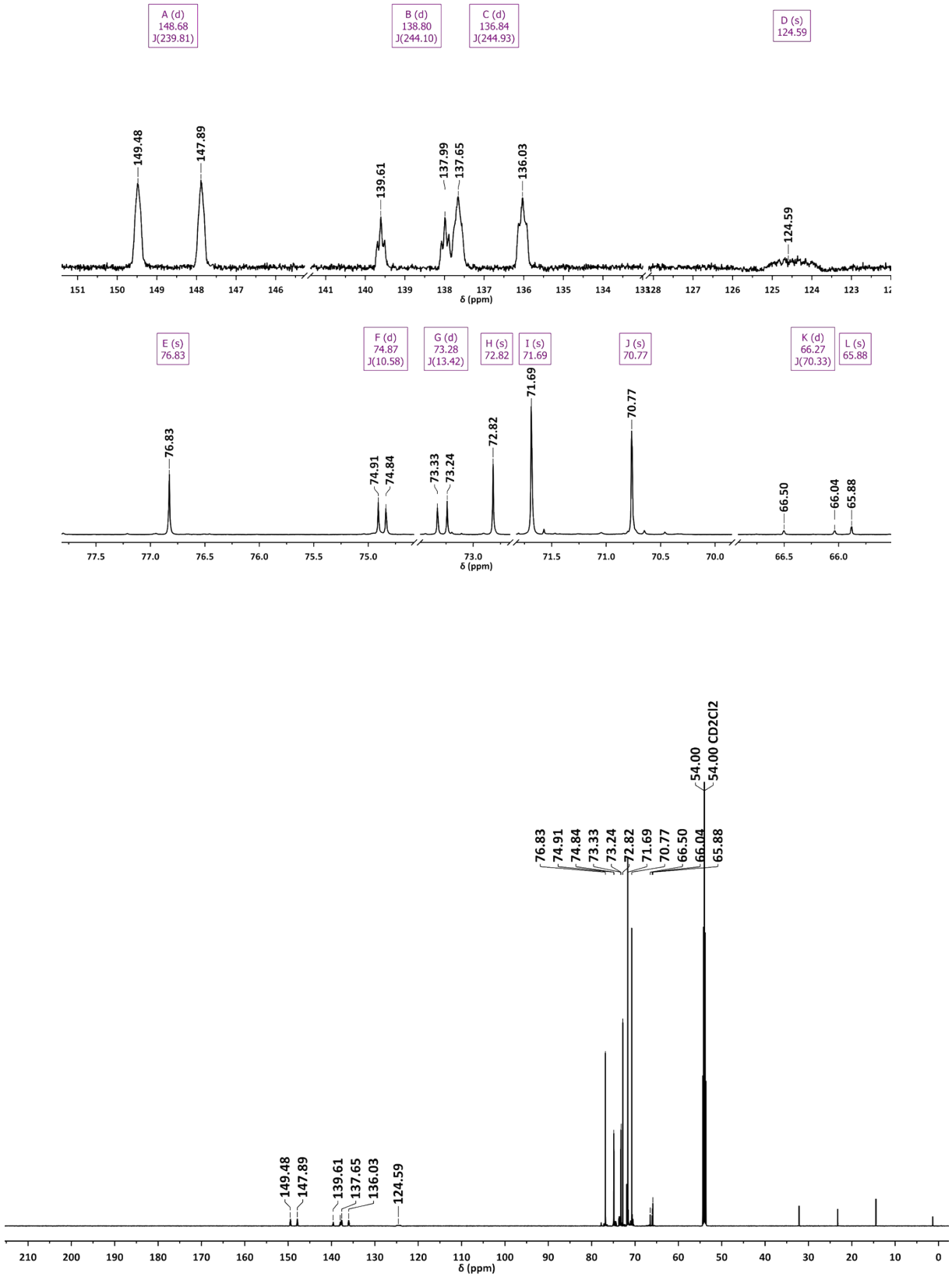

Figure S25. ^{13}C NMR (CD_2Cl_2, 151 MHz) spectra of $[Fc_2P(SeFc)_2][B(C_6F_5)_4]$ (**4**).

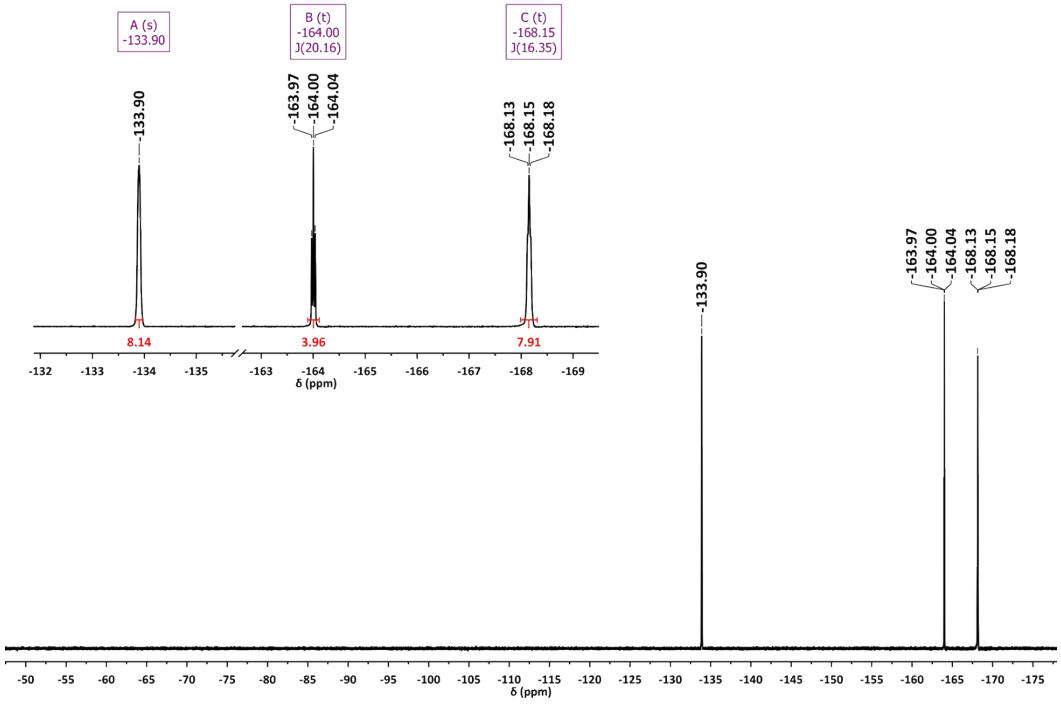

Figure S26. ^{19}F NMR (CD_2Cl_2, 565 MHz) spectrum of $[Fc_2P(SeFc)_2][B(C_6F_5)_4]$ (**4**).

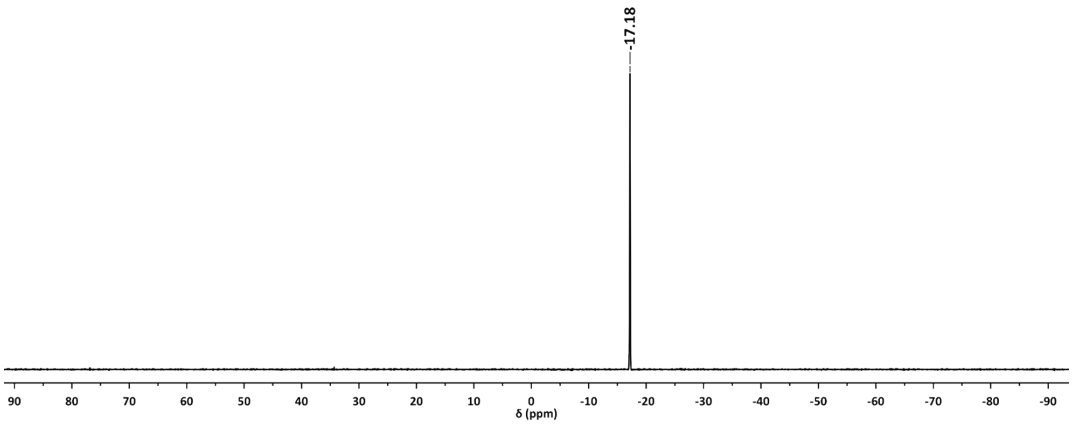

Figure S27. ^{11}B NMR (CD_2Cl_2, 193 MHz) spectrum of $[Fc_2P(SeFc)_2][B(C_6F_5)_4]$ (**4**).

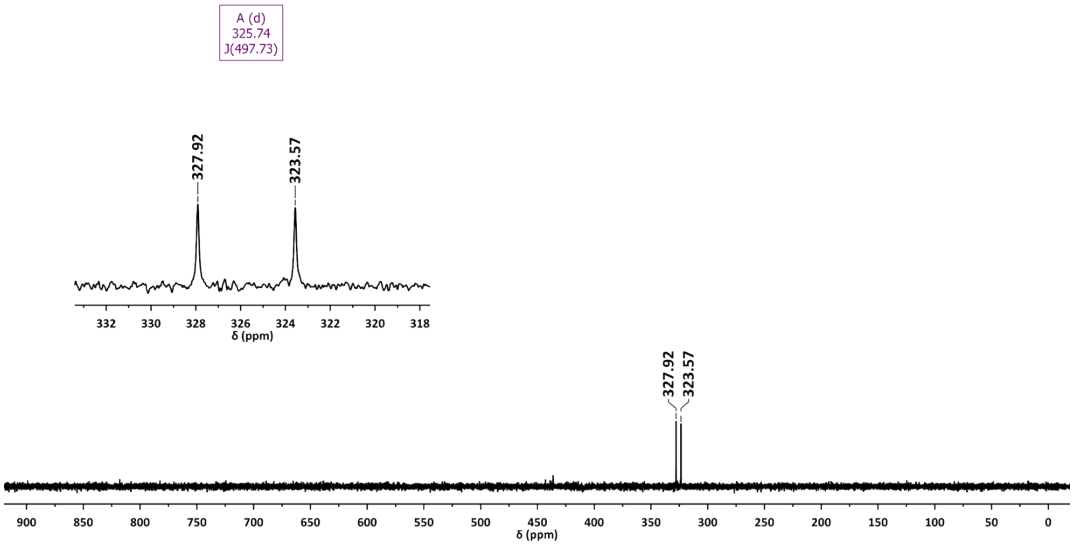

Figure S28. ^{77}Se NMR (CD_2Cl_2, 114 MHz) spectrum of $[Fc_2P(SeFc)_2][B(C_6F_5)_4]$ (**4**).

2.5 $[Fc_2P(Se_2biphen)][B(C_6F_5)_4]$ (5)

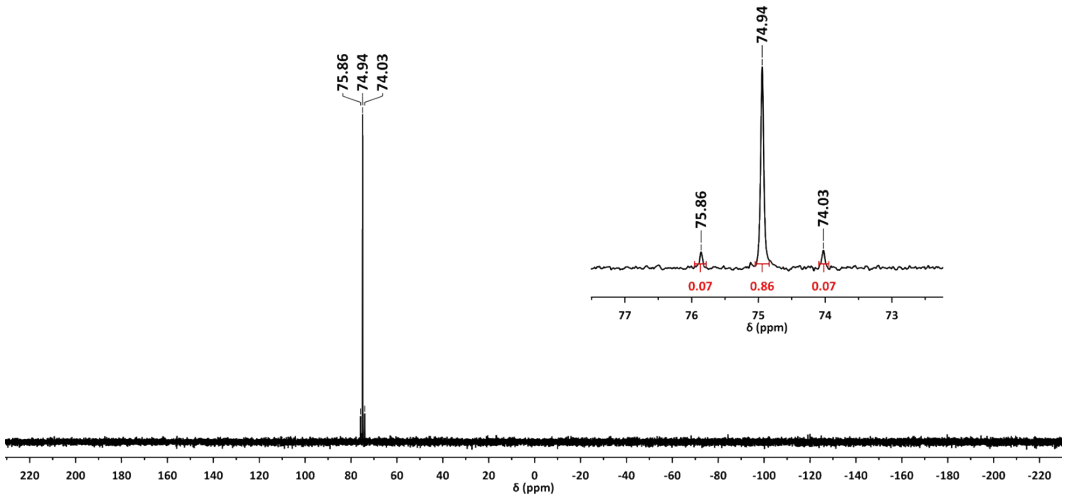

Figure S29. ^{31}P NMR (CD_2Cl_2, 243 MHz) spectrum of $[Fc_2P(Se_2biphen)][B(C_6F_5)_4]$ (**5**).

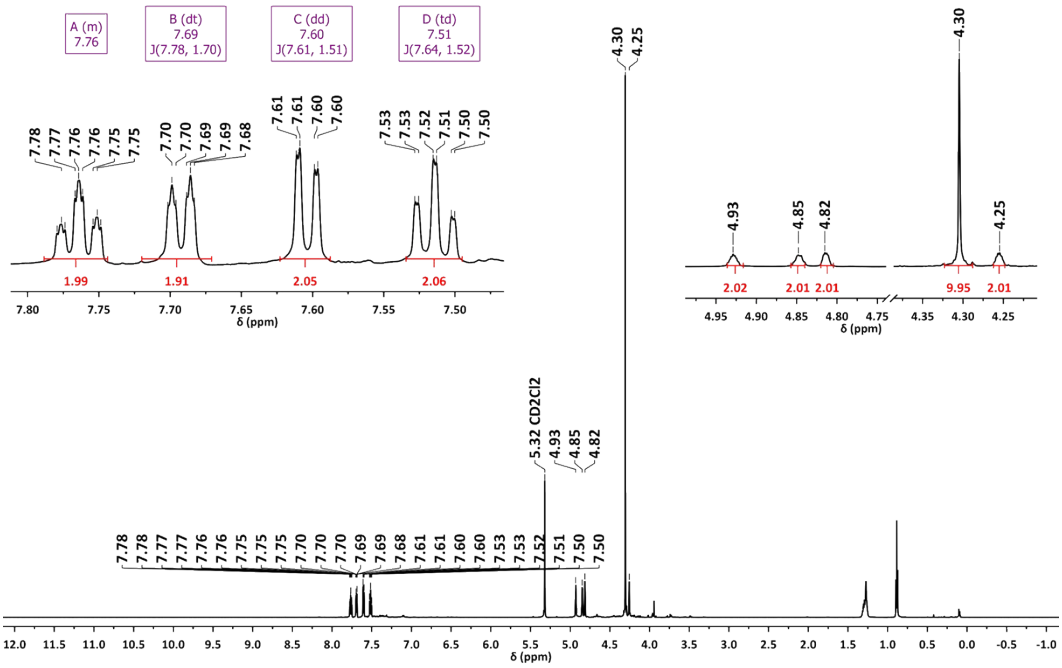

Figure S30. ^{1}H NMR (CD_2Cl_2, 600 MHz) spectrum of $[Fc_2P(Se_2biphen)][B(C_6F_5)_4]$ (**5**).

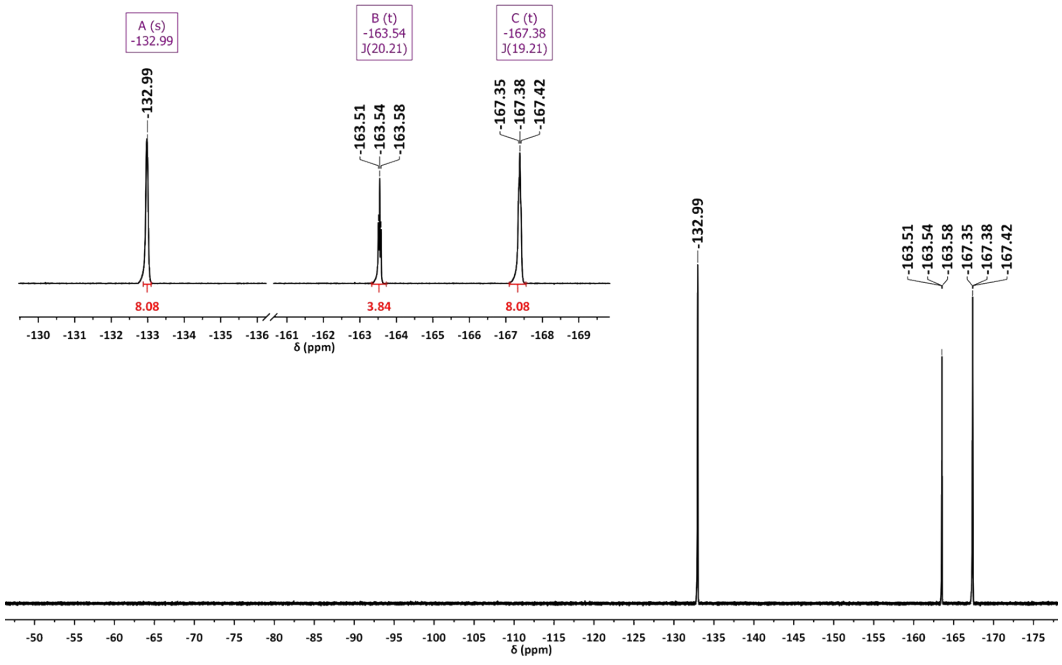

Figure S31. ^{19}F NMR (CD_2Cl_2, 565 MHz) spectrum of $[Fc_2P(Se_2biphen)][B(C_6F_5)_4]$ (**5**).

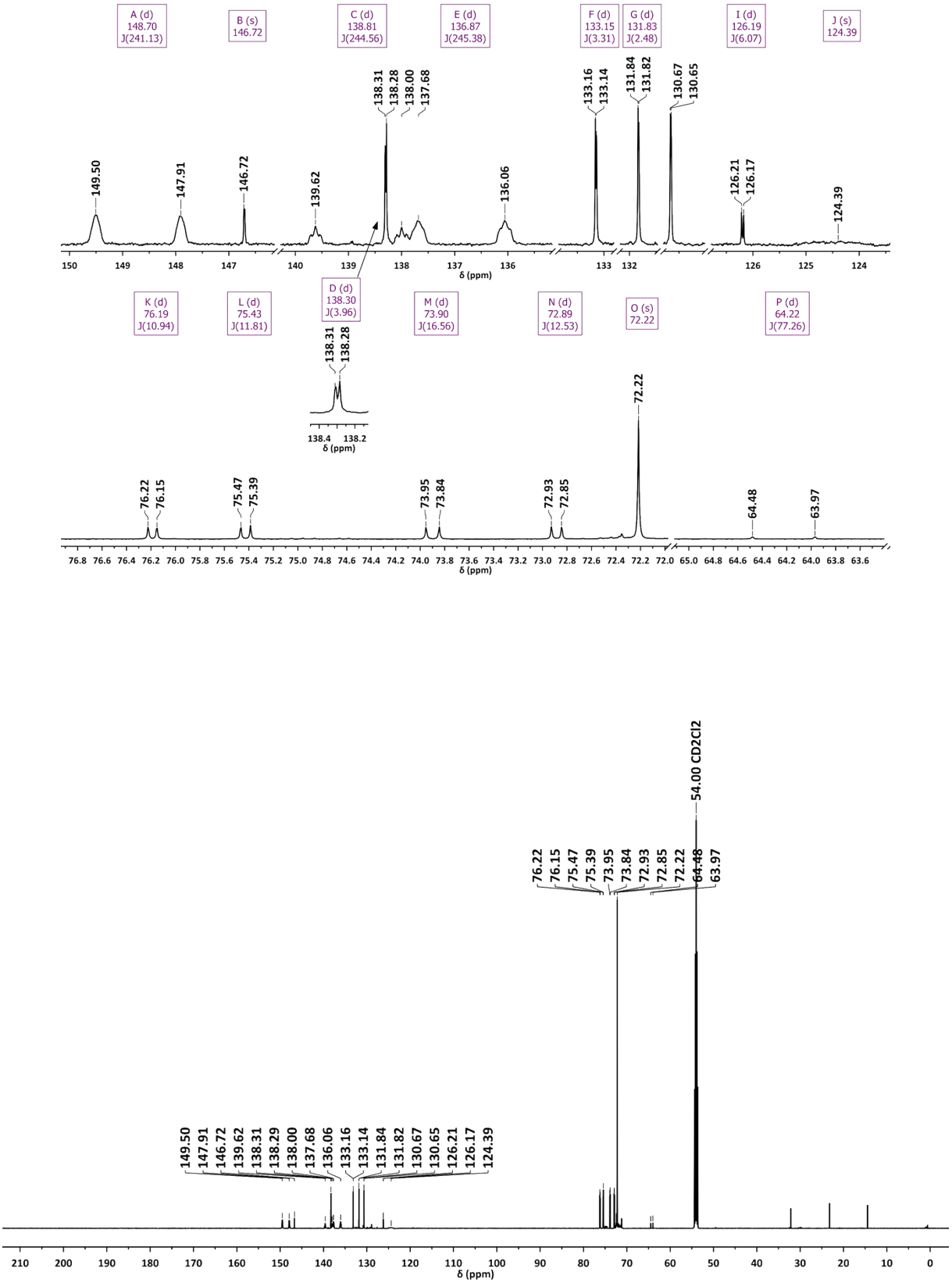

Figure S32. ^{13}C NMR (CD_2Cl_2, 151 MHz) spectra of $[Fc_2P(Se_2biphen)][B(C_6F_5)_4]$ (**5**).

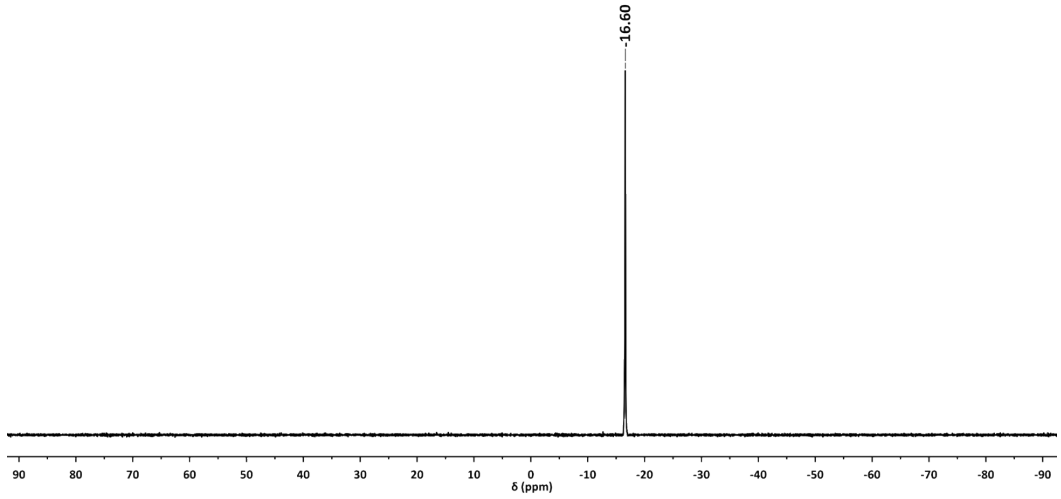

Figure S33. ^{11}B NMR (CD_2Cl_2, 193 MHz) spectrum of $[Fc_2P(Se_2biphen)][B(C_6F_5)_4]$ (**5**).

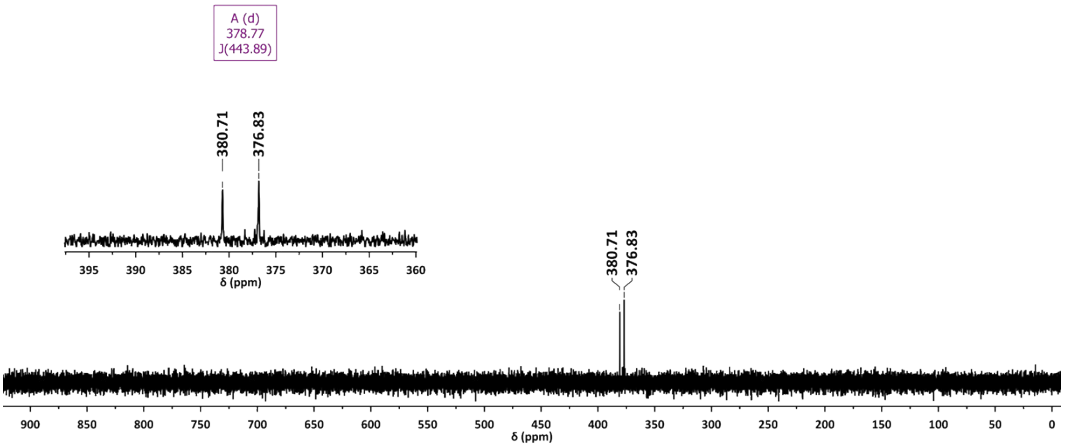

Figure S34. ^{77}Se NMR (CD_2Cl_2, 114 MHz) spectrum of $[Fc_2P(Se_2biphen)][B(C_6F_5)_4]$ (**5**).

3 Michael addition

3.1 General Procedure

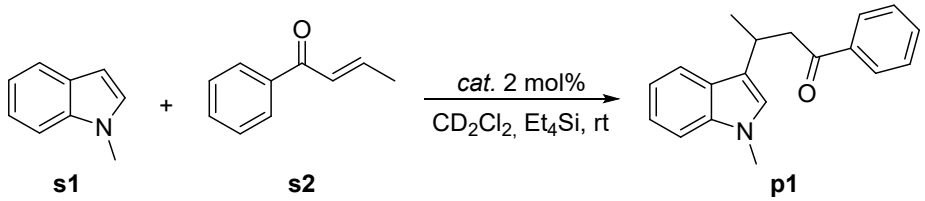

All experiments were carried on under inert conditions in a J. Young NMR tube and followed by NMR. The corresponding catalyst (compounds **1**–**5** or the $[Fc_2P][B(C_6F_5)_4]$ 40 µL, 0.6 µmol, 15 mM stock solution in CD_2Cl_2, 2 mol%) was added into the NMR-tube together with CD_2Cl_2 (100 µL). Then, it was followed by the addition of a 150 mM stock solution of *trans*-β-crotonophenone (**s2**, 200 µL, 30 µmol, 1.0 equiv., incl. 0.25 eq. Et_4Si) and a 150 mM stock solution of 1-methylindole (**s1**, 200 µL, 30 µmol, 1.0 equiv.), both in CD_2Cl_2. The tube was sealed, shaken and placed in an ultrasonic bath. After 30, 60 and 120 min of sonication, ^1H NMR measurements were conducted (4 scans, d_1 = 30 s, suitable for integration, assuming an error margin of 5%). The yields were determined by integration of the characteristic signal of product **p1** at 3.24 ppm (dd, *J* = 16, 8 Hz, 1H) and at 3.45 ppm (dd, J = 16, 5 Hz, 1H). The integral of the ethyl peak of Et_4Si (0.52 ppm, q, *J* = 8 Hz) was calibrated to *2* and/or the integral of the methyl peak of Et_4Si (0.94 ppm, t, *J* = 8 Hz) was calibrated to *3* against the starting material **s2**. Additionally, the consumption of the -CH_3 signal of **s2** at 2.00 ppm (dd, J = 7, 2 Hz, 3H) can be followed, together with the formation of the product **p1** with the characteristic -CH_3 signal at 1.42 ppm (d, J = 7 Hz, 3H).

Table S1. Catalytic screening of the Michael addition.

Catalyst (2 mol%)	*Conversion (yield) 30 min*	*Conversion (yield) 60 min*	*Conversion (yield) 120 min*
1	22 (10)	27 (16)	34 (22)
2	19 (10)	24 (12)	50 (38)
3	61 (50)	79 (68)	86 (74)
4	74 (62)	87 (78)	93 (86)
5	50 (36)	70 (56)	90 (78)
$[Fc_2P][B(C_6F_5)_4]$	100 (90)	-	-

Conversions and yields in %, as determined by ^{1}H-NMR (d1 = 30 s) using tetraethylsilane as internal standard.

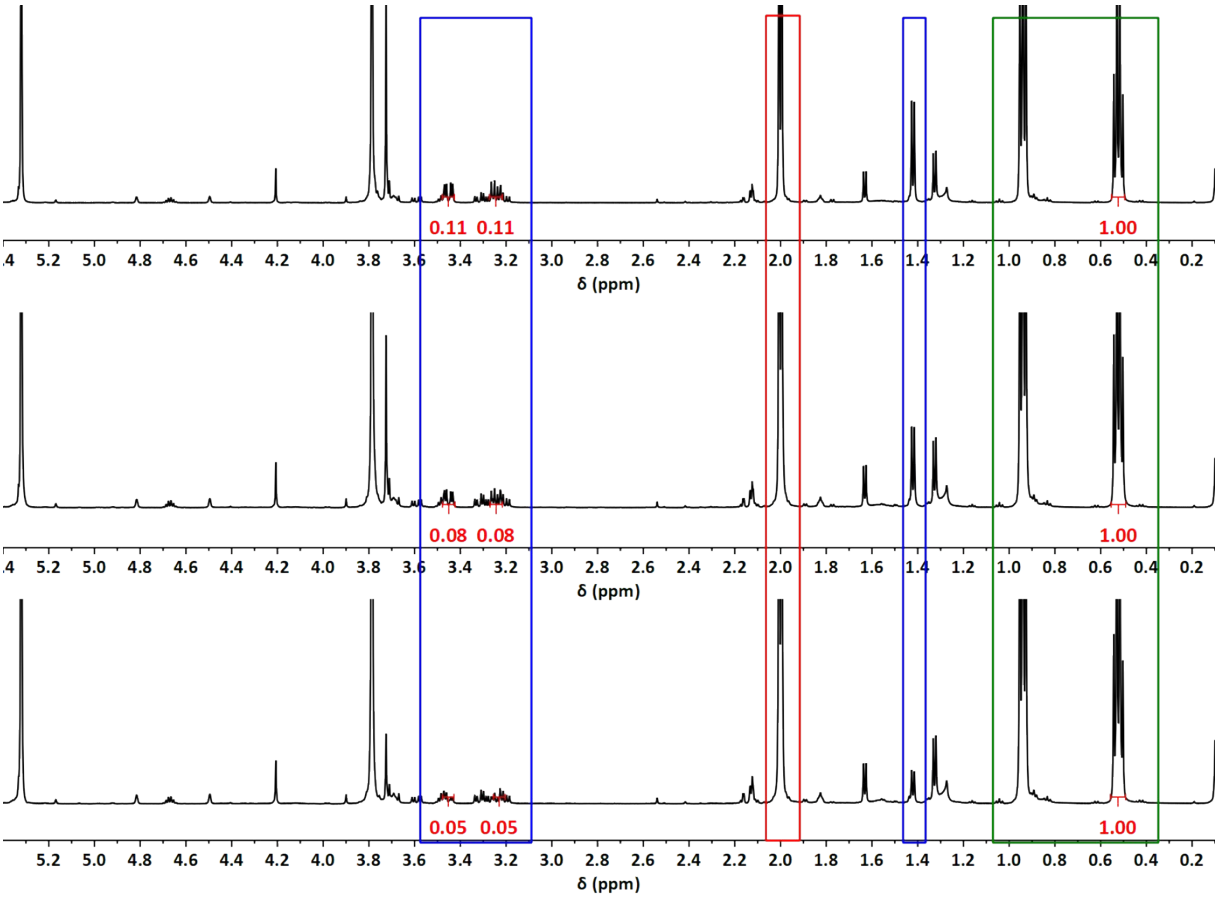

Figure S35. ^{1}H NMR (CD_2Cl_2, 600 MHz) spectra of the Michael addition using compound **1** as catalyst. Bottom to top: 30 min, 60 min and 120 min of sonication respectively. Important signals are marked as follows: blue for the newly formed product **p1**, red for **s2**, and green for Et_4Si.

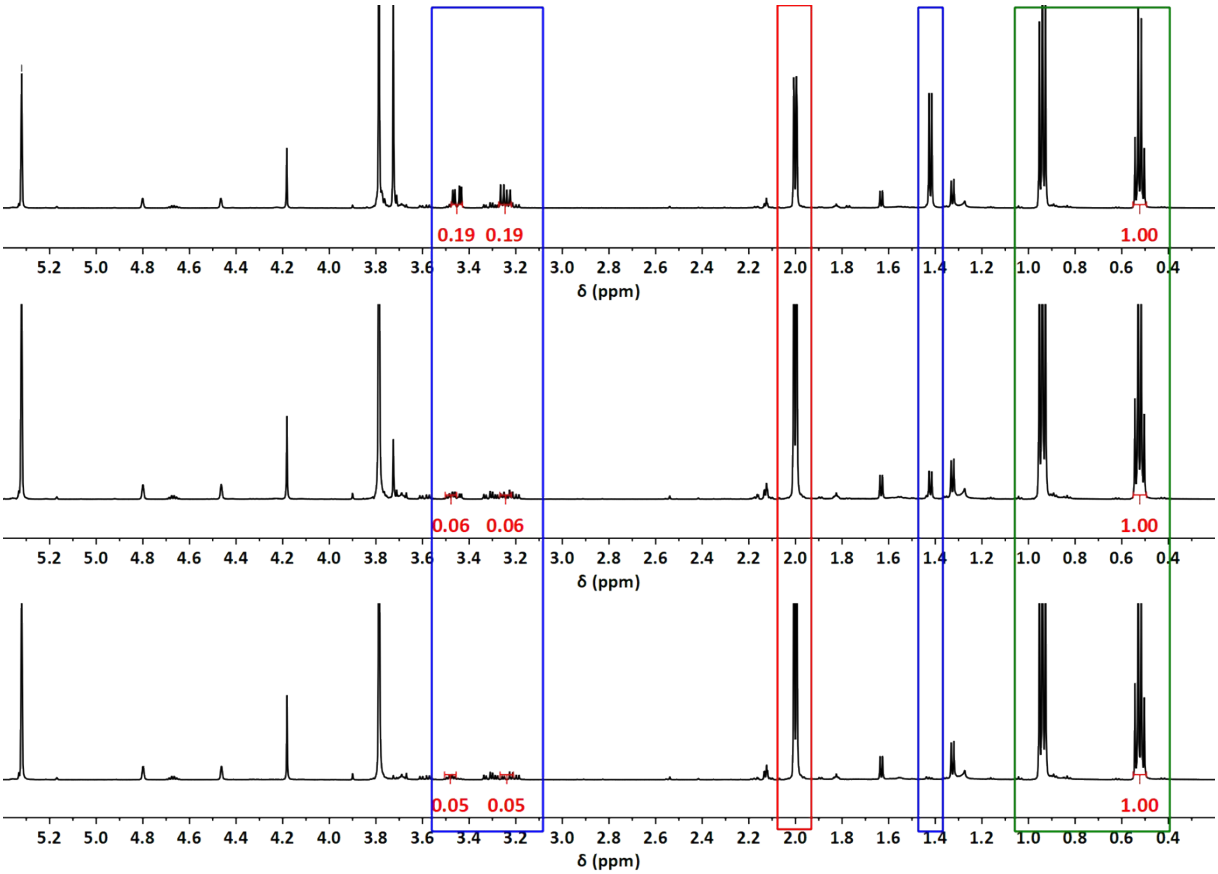

Figure S36. ^{1}H NMR (CD_2Cl_2, 600 MHz) spectra of the Michael addition using compound **2** as catalyst. Bottom to top: 30 min, 60 min and 120 min of sonication respectively. Important signals are marked as follows: blue for the newly formed product **p1**, red for **s2**, and green for Et_4Si. Full conversion (90% yield) after approximately 6 h of sonication.

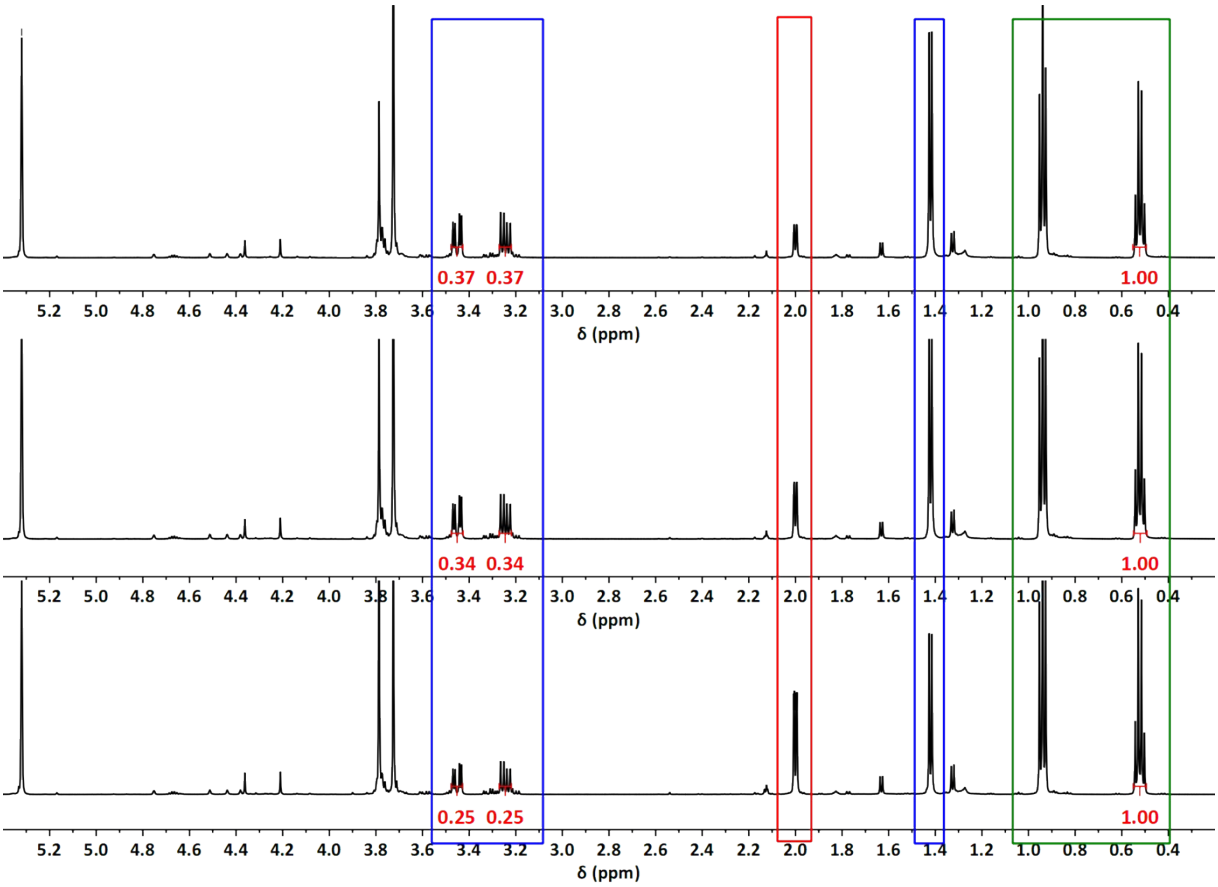

Figure S37. ^{1}H NMR (CD_2Cl_2, 600 MHz) spectra of the Michael addition using compound **3** as catalyst. Bottom to top: 30 min, 60 min and 120 min of sonication respectively. Important signals are marked as follows: blue for the newly formed product **p1**, red for **s2**, and green for Et_4Si. Full conversion (90% yield) after approximately 3 h of sonication.

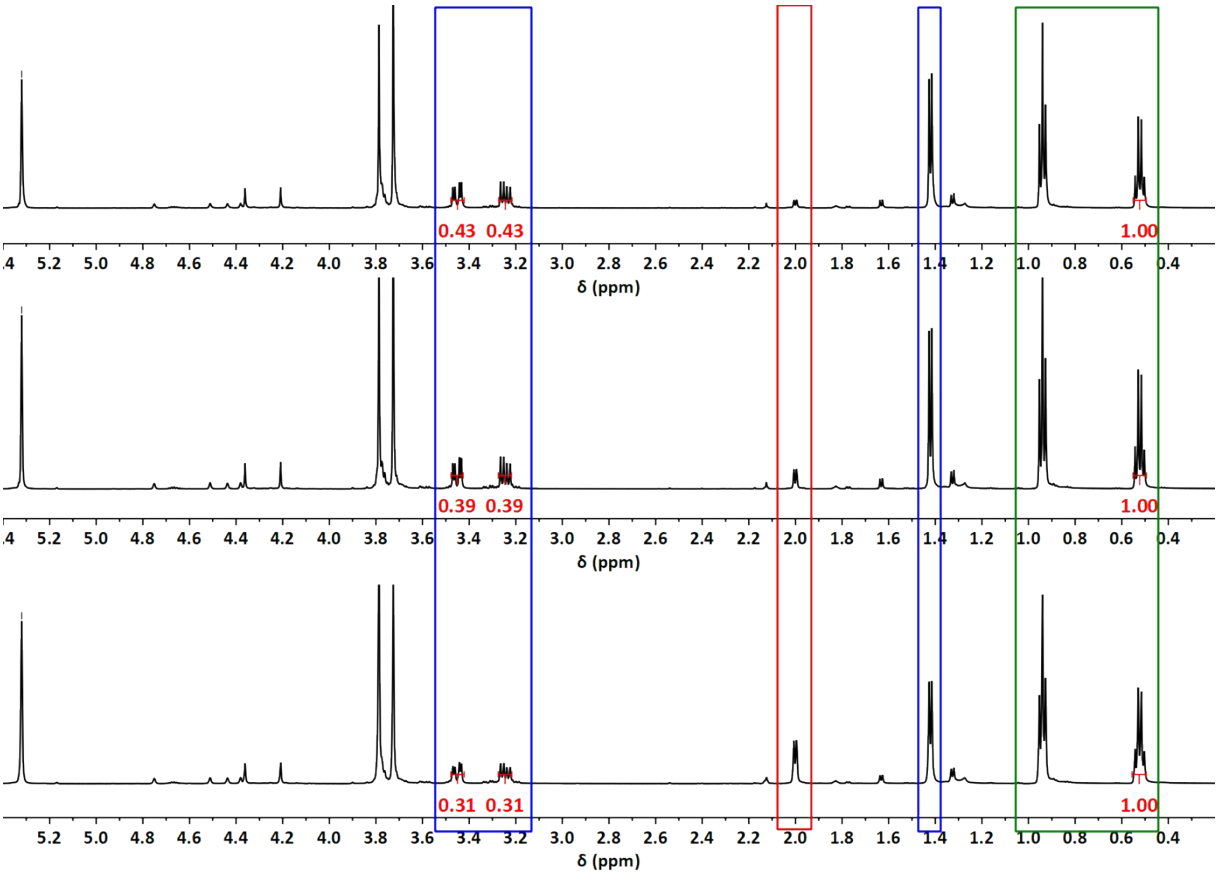

Figure S38. ^{1}H NMR (CD_2Cl_2, 600 MHz) spectra of the Michael addition using compound **4** as catalyst. Bottom to top: 30 min, 60 min and 120 min of sonication respectively. Important signals are marked as follows: blue for the newly formed product **p1**, red for **s2**, and green for Et_4Si. Full conversion (90% yield) after approximately 2.5 h of sonication.

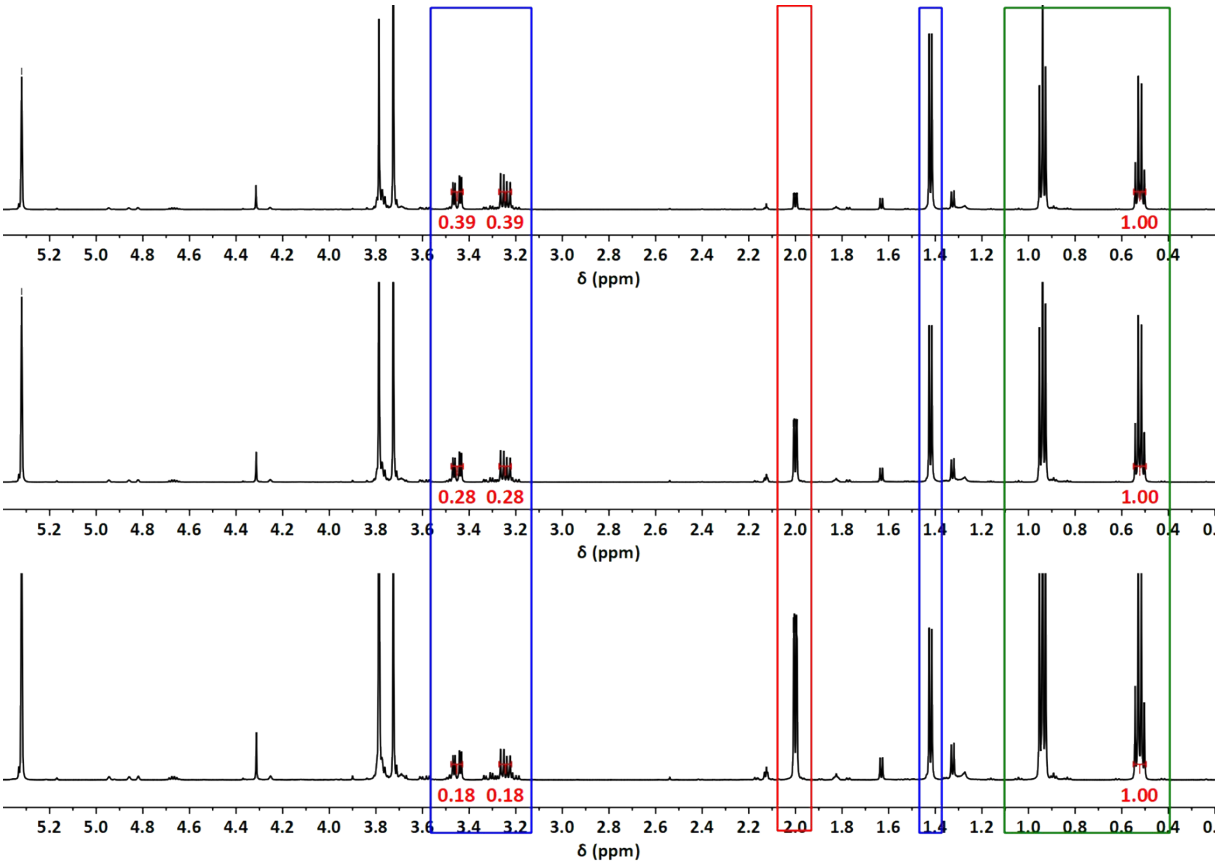

Figure S38. ^{1}H NMR (CD_2Cl_2, 600 MHz) spectra of the Michael addition using compound **5** as catalyst. Bottom to top: 30 min, 60 min and 120 min of sonication respectively. Important signals are marked as follows: blue for the newly formed product **p1**, red for **s2**, and green for Et_4Si. Full conversion (90% yield) after approximately 4 h of sonication.

4 Crystallographic Data

Intensity data of **1**–**5** was collected on a Bruker Venture D8 diffractometer at 100 K with graphite-monochromatic Mo-Kα (0.7107 Å) radiation. All structures were solved by direct methods and refined based on F^2 by use of the SHELX program package as implemented in WinGX[S6,S7] or OLEX2.[S8] All non-hydrogen atoms were refined using anisotropic displacement parameters. Hydrogen atoms attached to carbon atoms were included in geometrically calculated positions using a riding model. Crystal and refinement data are collected in Supplementary Tables S2 – S4. Figures were created using Diamond.[S9] Crystallographic data for the structural analyses have been deposited with the Cambridge Crystallographic Data Centre. Copies of this information may be obtained free of charge from The Director, CCDC, 12 Union Road, Cambridge CB2 1EZ, UK (Fax: +44-1223-336033; e-mail: deposit@ccdc.cam.ac.uk or http://www.ccdc.cam.ac.uk).

Table S2. Crystal data and structure refinement of compounds **1** and **2**.

	1	**2**
Formula	$C_{56}H_{28}BF_{20}Fe_2PS_2$	$C_{56}H_{28}BF_{20}Fe_2PSe_2$
Formula weight, g mol^{-1}	1298.38	1392.18
Crystal system	monoclinic	monoclinic
Crystal size, mm	0.40 × 0.30 × 0.10	0.40 × 0.40 × 0.40
Space group	C2/c	C2/c
a, Å	16.270(2)	16.240(2)
b, Å	16.235(2)	16.332(2)
c, Å	38.130(5)	38.510(5)
α, º	90	90
β, º	98.979(6)	98.942(4)
γ, º	90	90
V, Å^3	9949(2)	10090(2)
Z	8	8
ρ_{calcd}, Mg m^{-3}	1.734	1.833
μ (Mo *Kα*), mm^{-1}	0.816	2.165
F(000)	5184	5472
θ range, deg	2.27 to 28.70	2.43 to 27.10
Index ranges	–21 ≤ h ≤ 21	–23 ≤ h ≤ 24
	–21 ≤ k ≤ 21	–25 ≤ k ≤ 25
	–51 ≤ l ≤ 51	–59 ≤ l ≤ 59
No. of reflns collected	86690	96558
Completeness to θ_{max}	99.9%	99.9%
No. indep. Reflns	12851	19286
No. obsd reflns with ($I>2\sigma(I)$)	10879	15448
No. refined params	739	739
GooF (F^2)	1.142	1.046
R_1 (F) ($I > 2\sigma(I)$)	0.0489	0.0377
wR_2 (F^2) (all data)	0.1128	0.0872
Largest diff peak/hole, e Å^{-3}	1.232 / –0.584	0.568 / –0.507
CCDC number	2423663	2423664

Table S3. Crystal data and structure refinement of compounds **2**·toluene and **3**·CH_2Cl_2.

	2·toluene	**3**·CH_2Cl_2
Formula	$C_{63}H_{36}BF_{20}Fe_2PSe_2$	$C_{57}H_{30}BCl_2F_{20}Fe_2PTe_2$
Formula weight, g mol^{-1}	1484.32	1574.39
Crystal system	triclinic	triclinic
Crystal size, mm	0.21 × 0.20 × 0.18	0.50 × 0.19 × 0.16
Space group	$P\bar{1}$	$P\bar{1}$
a, Å	10.8629(8)	10.3907(6)
b, Å	15.1456(11)	15.4524(8)
c, Å	17.3801(10)	18.1339(9)
α, º	71.852(2)	104.965(2)
β, º	75.728(2)	103.652(2)
γ, º	87.113(3)	92.341(2)
V, Å^3	2632.3(3)	2717.3(3)
Z	2	2
ρ_{calcd}, Mg m^{-3}	2.081	1.924
μ (Mo *Kα*), mm^{-1}	1.873	1.824
F(000)	1468	1524
θ range, deg	2.37 to 27.50	2.03 to 27.50
Index ranges	–14 ≤ h ≤ 13	–13 ≤ h ≤ 13
	–19 ≤ k ≤ 19	–20 ≤ k ≤ 20
	–22 ≤ l ≤ 22	–23 ≤ l ≤ 22
No. of reflns collected	60562	122020
Completeness to θ_{max}	99.9%	99.9%
No. indep. Reflns	12070	12481
No. obsd reflns with ($I>2\sigma(I)$)	9204	12032
No. refined params	739	739
GooF (F^2)	1.057	1.099
R_1 (F) ($I > 2\sigma(I)$)	0.0441	0.0224
wR_2 (F^2) (all data)	0.1269	0.0568
Largest diff peak/hole, e Å^{-3}	0.748 / –0.585	0.912 / –0.956
CCDC number	2423665	2423666

Table S4. Crystal data and structure refinement of compounds **4** and **5**·CH_2Cl_2.

	4	**5**·CH_2Cl_2
Formula	$C_{64}H_{36}BF_{20}Fe_4PSe_2$	$C_{57}H_{28}BCl_2F_{20}Fe_2PSe_2$
Formula weight, g mol^{-1}	1608.03	1475.09
Crystal system	triclinic	monoclinic
Crystal size, mm	0.38 × 0.26 × 0.26	0.22 × 0.16 × 0.07
Space group	$P\bar{1}$	$P2_1/n$
a, Å	13.4185(6)	16.326(4)
b, Å	13.8756(6)	9.990(2)
c, Å	15.8321(7)	32.781(7)
α, º	100.509(2)	90
β, º	95.382(2)	98.502(9)
γ, º	92.036(2)	90
V, Å^3	2881.4(2)	5288.1(19)
Z	2	4
ρ_{calcd}, Mg m^{-3}	1.853	1.853
μ (Mo *K*α), mm^{-1}	2.387	2.169
F(000)	1584	2896
θ range, deg	2.39 to 30.52	2.40 to 28.32
Index ranges	–19 ≤ h ≤ 19	–21 ≤ h ≤ 21
	–19 ≤ k ≤ 19	–13 ≤ k ≤ 13
	–22 ≤ l ≤ 22	–43 ≤ l ≤ 43
No. of reflns collected	177357	98939
Completeness to θ_{max}	99.9%	99.8%
No. indep. Reflns	17580	13162
No. obsd reflns with ($I>2\sigma(I)$)	15978	10777
No. refined params	847	739
GooF (F^2)	1.063	1.039
R_1 (F) ($I > 2\sigma(I)$)	0.0299	0.0446
wR_2 (F^2) (all data)	0.0766	0.1266
Largest diff peak/hole, e Å^{-3}	1.083 / –1.069	0.982 / –0.797

CCDC number	2423667	2423668

5 Computational Details

Geometry Optimizations were carried out using density functional theory (DFT) using the B3PW91/6-311+G(2df,p)[S10,11] level of theory using the Gaussian16[S12] software package. For Se and Te effective core potentials accounting for 10 (Se) and 28 (Te) electrons and corresponding cc-pVTZ basis sets[S13] were used. Dispersion effects were modelled using Grimme's GD3BJ parameters.[S14] Electrostatic potentials were plotted with VMD.[S15]

6 References

[S1] C. Stoian, M. Olaru, S. Demeshko, M. Fischer, S. Mebs, E. Hupf, J. Beckmann, *Chem. Eur. J.* **2025,** *31*, e202403555.

[S2] M. Herberhold, P. Leitner, *J. Organomet. Chem.* **1987**, *336*, 153–161.

[S3] T. M. Klapötke, B. Krumm, M. Scherr, *Z. Anorg. Allg. Chem.* **2010**, *636*, 1955–1961.

[S4] G. R. Fulmer, A. J. M. Miller, N. H. Sherden, H. E. Gottlieb, A. Nudelman, B. M. Stoltz, J. E. Bercaw, K. I. Goldberg, *Organometallics* **2010**, *29*, 2176–2179.

[S5] F. Menges, "Spectragryph – optical spectroscopy software", Version 1.2.12, **2022**, http://www.effemm2.de/spectragryph/ (accessed 03.12.2024).

[S6] L. J. Farrugia WinGX suite for small-molecule single-crystal crystallography. *J. Appl. Crystallogr.* **1999***, 32***,** 837–838.

[S7] G. M. Sheldrick, *Acta Cryst.* **2015**, *C71***,** 3–8.

[S8] O. V. Dolomanov, L. J. Bourhis, R. J., Gildea, R. J., J. A. K. Howard, H. Puschmann, *J. Appl. Crystallogr.* **2009**, *42***,** 339–341.

[S9] Crystal Impact - Dr. H. Putz & Dr. K. Brandenburg GbR. *Diamond - Crystal and Molecular Structure Visualization,* 2014.

[S10] (a) A. D. Becke, *J. Chem. Phys.* **1993**, *98*, 5648−5652; (b) J. P. Perdew, J. A. Chevary, S. H. Vosko, K. A. Jackson, M. R. Pederson, D. J. Singh and C. Fiolhais, *Phys. Rev. B: Condens. Matter Mater. Phys.* **1992**, *46*, 6671–6687.

[S11] (a) R. Krishnan, J. S. Binkley, R. Seeger and J. A. Pople, *J. Chem. Phys.* **1980**, *72*, 650−654; (b) A. D. McLean and G. S. Chandler, *J. Chem. Phys.* **1980**, *72*, 5639–5648.

[S12] Gaussian16 (RevisionC.01), M. J. Frisch, G. W. Trucks, H. B. Schlegel, G. E. Scuseria, M. A. Robb, J. R. Cheeseman, G. Scalmani, V. Barone, G. A. Petersson, H. Nakatsuji, X. Li, M. Caricato, A. V. Marenich, J. Bloino, B. G. Janesko, R. Gomperts, B. Mennucci, H. P. Hratchian, J. V. Ortiz, A. F. Izmaylov, J. L. Sonnenberg, D. Williams-Young, F. Ding, F.

Lipparini, F. Egidi, J. Goings, B. Peng, A. Petrone, T. Henderson, D. Ranasinghe, V. G. Zakrzewski, J. Gao, N. Rega, G. Zheng, W. Liang, M. Hada, M.Ehara, K. Toyota, R. Fukuda, J. Hasegawa, M. Ishida, T. Nakajima, Y. Honda, O. Kitao, H. Nakai, T. Vreven, K. Throssell, J. A. Montgomery, Jr., J. E.Peralta, F. Ogliaro, M. J. Bearpark, J. J. Heyd, E. N. Brothers, K. N. Kudin, V. N. Staroverov, T. A. Keith, R. Kobayashi, J. Normand, K. Raghavachari, A. P. Rendell, J. C. Burant, S. S. Iyengar, J. Tomasi, M. Cossi, J. M. Millam, M. Klene, C. Adamo, R. Cammi, J. W. Ochterski, R. L. Martin, K. Morokuma, O. Farkas, J. B. Foresman and D. J. Fox, Gaussian, Inc., Wallingford CT, 2019.

[S13] (a) B. Metz, H. Stoll and M. Dolg, *J. Chem. Phys.* **2000**, *113*, 2563-2569; (b) K. A. Peterson, *J. Chem. Phys.* **2003**, *119*, 11099–11112. (c) K. A. Peterson, D. Figgen, E. Goll, H. Stoll and M. Dolg, *J. Chem. Phys.* **2003**, *119*, 11113–11123.

[S14] S. Grimme, S. Ehrlich and L. Goerigk, *J. Comp. Chem.* **2011**, *32*, 1456–1465.

[S15] W. Humphrey, A. Dalke and K. Schulten, *J. Mol. Graph.* **1996**, *14*, 33–38.